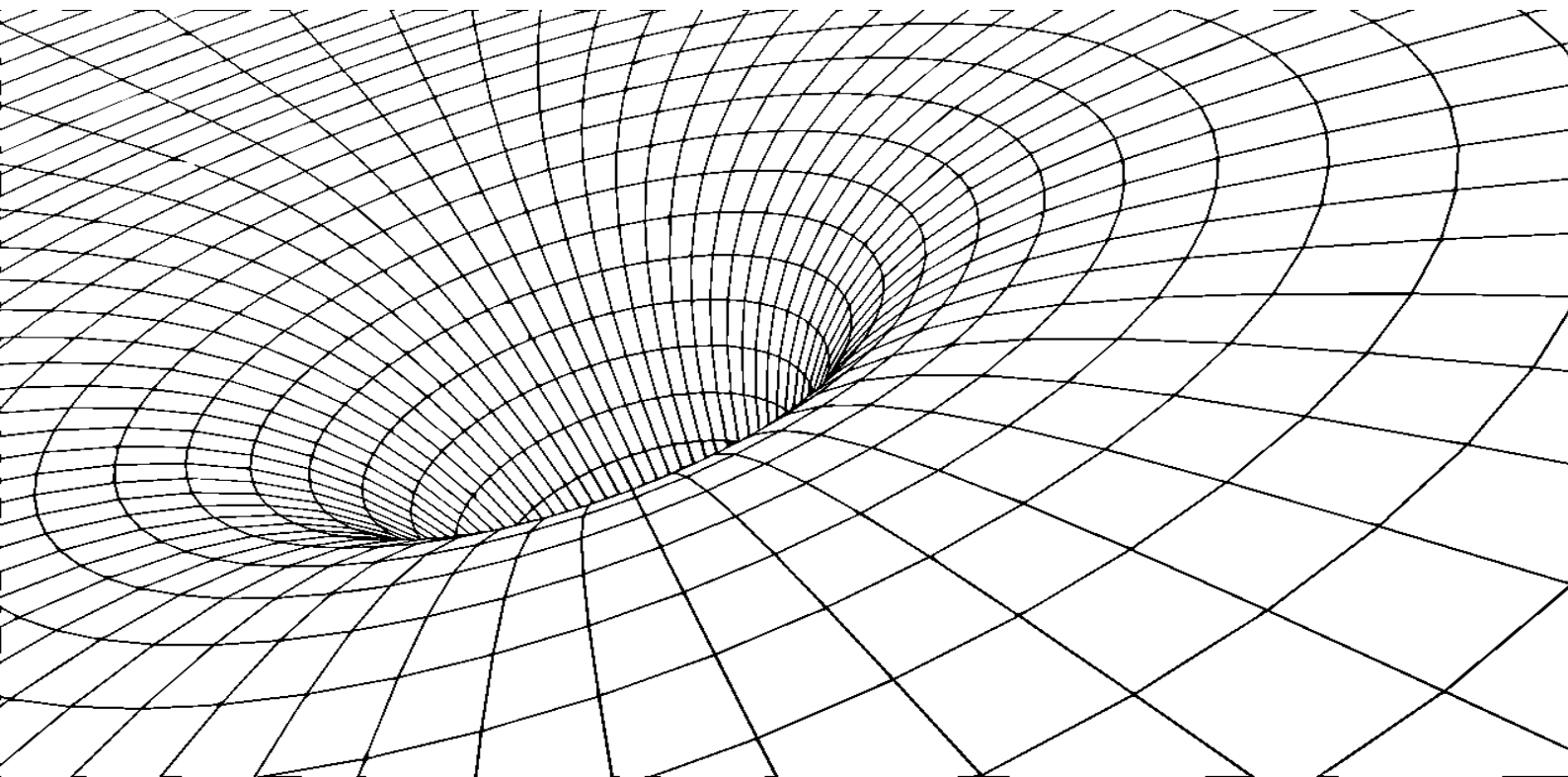


# BUSINESS-AS-USUAL AND ORBITAL DEBRIS PATH

Anelí Bongers and José L. Torres

University of Málaga



SPACE ECONOMICS

**Working Paper n. 08/2025**

# BUSINESS-AS-USUAL AND ORBITAL DEBRIS PATH

ANELÍ BONGERS

Department of Economics, University of Malaga, Spain

JOSÉ L. TORRES

Department of Economics, University of Malaga, Spain

Computing the so-called Business-as-Usual (BaU) scenario in Integrated Assessment Models (IAMs) that include environmental externalities is a non-trivial task. Traditionally, general equilibrium growth models with such externalities are solved in a centralized framework, where a social planner maximizes welfare by fully internalizing the environmental damage. This is the approach taken in the well-known DICE model by Nordhaus (1992). However, in DICE, the BaU scenario is defined as the planner's solution with zero abatement, even though the externality is already internalized through investment decisions to maximize social welfare. This creates a mismatch when comparing the BaU scenario to the true first-best allocation. This paper solves the DISE-2024 (Dynamic Integrated Space Economy) model in a decentralized economy, using a fixed point method to compute orbital debris trajectories under a *laissez-faire* setting, and compares them with the first-best optimal trajectories from a centralized economy. (JEL Classification: D62; E21; E22; Q53; Q58).

KEYWORDS. Orbital debris, Satellites, Integrated Assessment Models, Business-as-usual, Competitive decentralized equilibrium.

---

Anelí Bongers: [abongers@uma.es](mailto:abongers@uma.es)

José L. Torres: [jtorres@uma.es](mailto:jtorres@uma.es)

The authors gratefully acknowledge financial support from the Spanish Ministry of Science, Innovation, and Universities through Grant PID2023-152748OB-I00. The authors have no conflicts of interest or financial interests to disclose. Full replication code in GAMS is available from the authors under request.

## 1. INTRODUCTION

Computing the so-called Business-as-Usual (BaU) scenario, i.e., solving for a decentralized equilibrium in Integrated Assessment Models (IAMs) with environmental externalities, is not a trivial task. As noted by Shiell and Lyssenko (2008), simple optimization procedures tend to internalize the cost of pollution, which contradicts the very notion of BaU. Nevertheless, the literature frequently refers to the BaU scenario in climate-change IAMs, most notably in the DICE model (Nordhaus, 1992, 1993, 1998, 2018), as the reference trajectory that projects the future path of the economy without any new policy interventions, particularly without climate policies such as carbon taxes or emissions regulations, but under the assumption of a central planner maximizing social welfare.<sup>1</sup> In other models, simply the negative externality is ignored. However, a proper BaU scenario should reflect a setting in which agents act based solely on private incentives, without internalizing environmental externalities. It serves as the benchmark against which the costs and benefits of climate policy interventions are assessed.

These practices have led to a misunderstanding of the true meaning of the BaU scenario. On the one hand, if pollution damages are ignored, the BaU scenario overstates economic performance and can bias policy evaluations. A proper BaU should reflect the underlying market failure and their impact on the economy. On the other hand, models such as the standard DICE model are not computed as decentralized economies (Golosov et al., 2014). Instead, DICE is formulated as a social planner's problem, i.e., a centralized framework in which a benevolent planner maximizes aggregate social welfare over time. In this setup, the planner selects control variables such as consumption, investment, and possibly emissions abatement to maximize an intertemporal utility function, subject to the dynamic constraints of the economy and climate system. As a result, all externalities are fully internalized. This means the model does not capture the behavior of a real-world market economy in which decentralized agents act based on private incentives and ignore their impact on the climate. The direct implication is that the standard DICE outputs, such as the "optimal" carbon price or temperature trajectory, are not the result of decentralized individual decisions, but rather represent the first-best, socially optimal benchmark. In other words, DICE is solved as a normative, centralized optimization model that provides guidance on what should be done, not a positive model that describes what the economy would do on its own in the absence of policy.

In contrast, modeling a decentralized economy requires explicitly representing both firms and households as decision-makers who respond to private costs and benefits, without internalizing the environmental damage they cause. This setup must also include a market structure where emissions function as a negative externality. Within this framework, the competitive decentralized equilibrium can be extended to a Ramsey-style

---

<sup>1</sup>Other examples of climate-change IAMs where the economy module is formalized with a micro-founded general equilibrium model are the ETA-MACRO (Model of Energy-Economy Interactions) by Manne (1977), the GLOBAL-2100 model of Manne and Richels (1992), the CETA (Carbon Emissions Trajectory Assessment) model by Peck and Teisberg (1992), the MERGE (Model for Evaluating Regional and Global Effects) model by Manne et al., (1995), or the work of Golosov et al. (2000).

second-best allocation by introducing policy instruments, such as Pigouvian taxes or cap-and-trade systems, to partially correct for the externality. The key insight is that, in a decentralized economy, the social cost of environmental damage is not automatically internalized. Instead, it influences the optimal behavior of private agents only if appropriate policy mechanisms are in place. This creates a feedback loop: private decisions affect the environment, and environmental degradation, in turn, shapes future economic outcomes. Accurate capture of this interaction is essential for evaluating the effectiveness and welfare implications of environmental policy.

A different challenge arises when the Integrated Assessment Model (IAM) is not global, but instead consists of multiple regions. In this case, there is more than one agent contributing to the environmental externality, and emissions by one agent affect others as well. This is the structure used in models such as RICE (Nordhaus and Yang, 1996; Nordhaus and Boyer, 2000; Yang, 2003) and in Krusell and Smith (2024). In a multi-region setting, the central planner's solution corresponds to the Nash equilibrium of a non-cooperative game in which each region internalizes only the damages it imposes on itself, while ignoring the external effects of its emissions on other regions. As a result, the externality is only partially internalized, even in the so-called planner's solution. However, a similar conceptual misunderstanding occurs in Nordhaus and Yang (1996), Nordhaus and Boyer (2000) and Yang (2003), where the BaU scenario is identified with the outcome of a regional-level social planner who does not implement any emissions abatement policy. This approach again conflates a partially internalized externality with a truly decentralized market outcome. By contrast, Krusell and Smith (2024) correctly address the issue by computing the BaU scenario as the outcome of a competitive equilibrium, in which each agent acts based solely on private incentives, fully ignoring the external effects of their emissions and considering damages as exogenous.

In the literature, there have been several efforts to “decentralize” IAMs in environmental economics, such as the well-known DICE model, by adopting market-based frameworks (e.g., competitive decentralized general equilibrium models with pollution externalities) in which emissions are not internalized by private agents. This approach enables the construction of BaU scenarios or policy counterfactuals that reflect decentralized behavior. It also allows for meaningful comparisons between decentralized equilibria and the central planner's solution, thereby quantifying the potential welfare gains from regulation. Notable examples of this approach include Shiell and Lyssenko (2008), Golosov et al. (2014), Hassler et al. (2021), and Krusell and Smith (2024).

This paper follows the recent strand of literature that models decentralized economies within Integrated Assessment Models (IAMs). Specifically, it employs a fixed-point algorithm to solve for the decentralized equilibrium, interpreted as the BaU or *laissez-faire* scenario, in the DISE-2024 model (Bongers and Torres, 2025). DISE-2024 is a global IAM focused on the space environment, where the environmental externality takes the form of orbital debris. Satellite launches and orbital operations generate debris that can collide with functioning satellites, often with catastrophic consequences. Moreover, large objects such as derelict satellites and spent rocket stages can fragment into thousands of smaller

pieces through breakups or explosions.<sup>2</sup> The presence of orbital debris introduces a negative externality, causing a divergence between private and social costs. As a result, competitive equilibrium allocations are inefficient. In this context, the private returns to space capital (e.g., satellites) do not fully account for the environmental costs imposed on the orbital commons. Agents thus perceive the returns to satellite investment as higher than they are from a social perspective, leading to overinvestment in space capital relative to the social optimum.

The basic idea of our approach is similar to that used by Krusell and Smith (2024) in the context of climate change. Krusell and Smith (2024) propose a fixed-point iteration method to compute the competitive equilibrium. The method begins with initial guesses for the global temperature trajectory and the sequence of regional transfer payments (e.g., from carbon taxes). They then solve the Bellman equation backward in time to derive time-dependent decision rules (policy functions). Using these rules, they simulate the economy forward, producing updated paths for global capital, consumption, emissions, and temperature. This procedure is repeated until the initial guesses and the resulting trajectories converge, achieving a fixed point that represents a consistent decentralized equilibrium.

In this paper, we adopt a similar fixed-point strategy, but instead frame the model as a nonlinear programming problem. In each iteration, the optimal path of economic and environmental variables is computed under the assumption that the environmental externality is not internalized. Starting from an initial guess for the trajectory of orbital debris and its associated damages, we solve the optimal growth model over a given time horizon to obtain a new debris and damage trajectory. This updated externality path is then fed back into the model, which is re-optimized. The process is repeated iteratively until the damages converge to a fixed point, ensuring consistency in the decentralized equilibrium. The *laissez-faire* trajectories for the main variables are compared to the social planner's trajectories as a benchmark for investigating optimal orbital debris mitigation policies.

The remainder of the rest of the paper is organized as follows. Section 2 present the model for a decentralized economy. In Section 3, a global economy-space model is developed to show the relationship between the final output of the World economy and the amount of satellites in a space environment affected by orbital debris. Section 4 presents the competitive decentralized solution whereas Section 5 presents the decentralized solution algorithm. In Section 6, the model is calibrated. Section 7 presents the main results from the simulation of the model. Finally, Section 8 presents some conclusions.

## 2. RELATED LITERATURE

The literature has addressed this issue by developing alternative approaches for computing decentralized equilibria in the presence of negative externalities. Shiell and Lyssenko

---

<sup>2</sup>A particularly concerning feature of orbital debris is its self-reinforcing nature: collisions generate debris fragments that, in turn, increase the likelihood of further collisions. This feedback loop leads to an endogenous process of debris accumulation, a phenomenon known as the "Kessler Syndrome" (Kessler and Cour-Palais, 1978; Kessler, 1991). Over time, it may render entire orbital regions unusable.

(2008) propose one such method, the so-called *N*-agent approach, to construct a BaU scenario in a dynamic general equilibrium model with a pollution externality. They identify a key problem in standard IAMs: even when attempting to model a no-policy world, pollution costs are often unintentionally internalized due to the optimization framework used. To overcome this, Shiell and Lyssenko (2008) simulate the economy as composed of many identical agents, each of whom acts in their own self-interest while ignoring their negligible individual impact on the environment. As the number of agents becomes large, the aggregate outcome approximates a setting where the externality is fully uninternalized, i.e., a true market failure. This approach generates a BaU trajectory that accurately reflects the decentralized behavior of economic agents and provides a more appropriate baseline for evaluating the costs and benefits of climate policy.

Rezai (2010) argues that the original DICE model's BaU scenario is flawed because it assumes zero abatement and ignores pollution damages, making climate policy appear costly and intergenerationally unfair. By correcting the BaU to reflect marginal damages from emissions, Rezai shows that early and strong mitigation is not a sacrifice but a Pareto improvement that benefits both current and future generations. Rezai (2011) argues that the perceived cost of climate policy hinges on the choice of BaU as a reference point. Traditional BaU scenarios assume no climate regulation and thus reflect an inefficient market outcome with excessive investment in polluting capital. He shows that comparing climate policy to this flawed baseline overstates its opportunity cost, whereas using an efficient, internalized baseline reveals that mitigation can increase overall welfare and avoid unnecessary overinvestment in dirty technologies. Rezai et al. (2012) argue that the standard BaU scenario, defined by a hybrid constrained optimal path, mischaracterizes the true economic baseline by ignoring uncorrected greenhouse gas externalities. When the BaU is properly understood as an inefficient equilibrium with excess pollution investment, internalizing emissions through mitigation shows no opportunity cost: diverting resources from conventional investment to climate action raises welfare for both current and future generations, yielding a Pareto improvement.

Nordhaus and Boyer (2000) solve the RICE99 model (an extension of the RICE model by Nordhaus and Yang (1996) with an energy supply module) for a decentralized setting. The decentralized (non-cooperative) equilibrium is solved by setting up the optimization problem for each region and solving them simultaneously as a static Nash equilibrium at each time point, that is, they set up a system of simultaneous optimality conditions and solve for all regions together, effectively solving for the Nash equilibrium in one large optimization problem.

Other authors calculate the paths for the competitive decentralized economy but assuming that the behavior of households and firms is independent from the environmental externality, that is, they do not adjust their behavior depending on the externality damages. This is the case of IAMs where the economy is exogenous (they are not based in the optimal growth model), or models where the environmental externality is fully ignored.

An alternative approach is provided by the analysis of Golosov et al. (2014). They develop a dynamic stochastic general equilibrium (DSGE) model that incorporates climate damages, where households and firms act in a decentralized manner, and the government

imposes a Pigouvian carbon tax to internalize the externality. The authors derive conditions under which the optimal carbon tax path replicates the planner's solution. Under a specific set of assumptions (logarithmic utility, Cobb-Douglas production, 100% capital depreciation, and climate damages that reduce total factor productivity), the saving rate becomes exogenous. In this framework, agents do not respond to the externality as a result of optimization, but rather because the externality is effectively neutralized in their decision-making. Intuitively, a future decline in TFP due to emissions creates two offsetting effects: a substitution effect that discourages saving (since the return to saving falls), and an income effect that encourages saving (because lower future productivity makes the future poorer). Under the stated assumptions, these effects exactly cancel out. A similar strategy is employed by Hasslet and Krusell (2012) for a multi-region model, and by Hassler et al. (2021) to evaluate the consequences of suboptimal climate policy by examining the effects of setting carbon taxes at incorrect levels.

Finally, Krusell and Smith (2024) models a multi-region economy with heterogeneous agents (regions) and computes decentralized equilibrium paths where regions act non-cooperatively. Their BaU scenario is computed using a fixed-point algorithm for a decentralized equilibrium. Each region maximizes utility without taking into account climate damages. Damages are computed and evolve, but do not enter agents' objective functions. This yields a realistic BaU path that reflects market failure due to climate inaction.

### 3. THE MODEL

This section describes the structure of the DISE-2024 model (Bongers and Torres, 2025). The model is a global space-economy model that covers not only the planet Earth but also the outer space. The DISE-2024 model has a similar general structure to climate-change IAMs but adapted to the particular characteristics of the outer space environment and specifically designed to study the economic and welfare implications of orbital debris. As standard climate-change AIMs, the DISE-2024 model is a combination of two sub-models: an economy model and an environmental model of pollution in the space. Emissions of debris, in-orbit endogenous generation of debris, and damage functions link the two sub-models.

The economic part is represented by an optimal growth model for the world economy comprising two capital inputs, where "satellites" are an additional type of capital in the aggregate production function. It is based on the neoclassical general equilibrium growth model initially developed by Ramsey (1928), further developed by Koopmans (1963) and Cass (1965). The model includes a negative externality that emerges from the pollution of outer space with orbital junk.<sup>3</sup> Unlike standard environmental economic models, pollution does not directly reduce output by reducing aggregate productivity. The cost of pollution on Earth's orbit comes from the fact that orbital debris increases the risk of collision and destruction of operational satellites. This, in turn, reduces the stock of in-orbit equipment and thus indirectly reduces production if the destroyed equipment is not replaced

---

<sup>3</sup>Orbital debris is not the only existing externality in Earth's orbit. Other externalities are congestion at particular altitudes, electromagnetic pollution, and radio-spectrum interference of nearby satellites. The DISE-2024 model focuses on pollution by orbital debris.

or reduces available resources for alternative uses in the case of replacement. In addition, the externality can impact economic growth, by affecting capital investment, both in the space and in the Earth, and the stock of capital in future periods.

The physical part of the model is represented by a tractable aggregate orbital debris evolutionary model that accounts for all types of debris emissions, with the exception of intentional debris emissions. As with the economy, the space model is also a global model for all orbits, from LEO to GEO. Together with the population of operational satellites (and other spacecraft, including two space-stations) we consider the dynamics of the population of orbital debris. The population of debris considered are objects greater than 1 cm. Debris are divided into three types: Derelict non-deorbited dead satellites, rocket bodies, and fragments. A key characteristic of the model is that dead satellites and rocket bodies can breakup either by internal factors or by collision with other objects, generating additional fragments.

One particular characteristic of DISE-2024 is that the model includes variables that are defined in two dimensions: physical variables and output-measured variables. We consider a mapping between physical variables of the space sector (i.e., number of satellites, number of satellites destroyed by collision) and the corresponding variables of the economic model (i.e., the value of satellite assets). Physical variables are represented in capital letters, while economic output-measured variables are represented in lowercase letters.

### 3.1 The economy model

The economy part of the model is based on the Ramsey (1928) optimal neoclassical growth model tailored to consider human activity in space. Time is discrete running to an infinity horizon.

**3.1.1 Households** The economy is inhabited by a large number of infinity-lived identical households. There is a representative household with instantaneous utility  $U(\hat{c}_t, N_t)$ , defined over per capita consumption  $\hat{c}_t$ , and where  $N_t$  is population. The aggregate consumption,  $c_t$ , is defined as  $c_t = \hat{c}_t N_t$ . The function  $U(\hat{c}_t, N_t)$  is the flow of utility which it is assumed to represent social well-being. The function  $U(\cdot)$  is assumed to be concave and twice continuously differentiable.

The problem to be solved by the stand-in household consists in choosing the optimal consumption path that maximizes the sum of discounted utility,

$$\max_{\{\hat{c}_t\}_{t=0}^{\infty}} \sum_{t=0}^{\infty} \left( \frac{1}{1+\rho} \right)^t U(\hat{c}_t, N_t) \quad (1)$$

where  $\rho > 0$  is the subjective intertemporal preference parameter or the pure rate of social time preference. The social discount factor,  $0 < \beta < 1$ , is defined as  $\beta = 1/(1+\rho)$ . There is a continuum of identical households, each of whom has preference that are characterized by the following instantaneous constant relative risk-aversion (CRRA-type) utility function,

$$U(c_t, N_t) = \left( \frac{\hat{c}_t^{1-\sigma} - 1}{1-\sigma} \right) N_t \quad (2)$$

where the parameter  $\sigma > 0$  represents the intertemporal marginal consumption elasticity also equal to the relative risk aversion. For the case in which  $\sigma = 1$ , the utility transforms in a logarithmic function. The parameter  $\sigma$  can also be interpreted as a measure of social aversion to changes in consumption (Nordhaus, 1993). Households are assumed to have an inelastically labor supply.

This household satisfies the following budget constraint,

$$c_t + i_t^k + i_t^s = r_t^k k_t + r_t^s s_t + w_t N_t + \pi_t \quad (3)$$

where  $i_t^k$  is investment in physical capital other than satellites (Earth capital),  $i_t^s$  is investment in satellites (space capital), which also include all costs to insert satellites into orbit, and  $y_t$  is final output. The rental rate of Earth capital is  $r_t^k$ , the rental rate of satellites is  $r_t^s$ , and  $w_t$  is labor income. They also receive dividends,  $\pi_t$ . All prices are defined in output units and normalized to one.

Inserting a satellite into orbit requires the use of a launch vehicle, which is costly. As a result, not all space investment spending is converted into productive space capital. To account for this, investment in space capital is divided into two components:

$$i_t^s = h_t + l_t \quad (4)$$

where  $h_t$  is the cost of satellites, and  $l_t$  is the cost of launch. The launch cost is interpreted as an installation cost necessary to build up the stock of satellites. To deploy a satellite capable of providing services, a launch vehicle must be used. This launch cost is modeled as a fixed adjustment cost per unit of investment, reflecting the fact that launch prices are typically fixed per kilogram of satellite mass, though they may vary depending on the target orbit. Alternatively, the launch cost can be viewed as a wedge or premium over the purchase price of space capital.

The Earth capital accumulation process is the standard inventory equation:

$$k_{t+1} = (1 - \delta_k)k_t + i_t^k \quad (5)$$

where  $0 < \delta_k < 1$  is the Earth capital depreciation rate.

The stock of satellites, measured in final output units as an equipment asset, is denoted by  $s_t$ , and is given by the following process,

$$s_{t+1} = (1 - \delta_s)s_t + q_t h_t - x_t \quad (6)$$

where  $0 < \delta_s < 1$  is the depreciation rate for satellites, and  $x_t$  is the loss of satellites assets by collisions (damage from space pollution) to be defined later. This accumulation process establishes the link between the space environment and economic activity. Damage results in the destruction of satellites, the reduction of space capital stock used in production, and the reduction of the final output if the loss asset is not replaced. The stock of satellites law of motion incorporates an investment-specific technological change component (ISTC), denoted by  $q_t$ , (see Greenwood et al., 1997). For simplicity, it is assumed that ISTC only occurs in the space sector.<sup>4</sup>

<sup>4</sup>ISTC captures the efficiency of investment in satellites, that is, is a measure of capital quality (embodied technology) per unit of investment spending in space assets, defined as the price of satellite goods relative to other consumption and Earth capital goods.

3.1.2 *Firms* We assume that all firms have access to the same technology, so we use a representative firm and a representative aggregate production function. Output is assumed to be a Cobb-Douglas type function of aggregate productivity, the stock of physical capital in the Earth,  $k_t$ , the stock of satellites,  $s_t$ , and labor,  $N_t$ ,

$$y_t = a_t k_t^{\alpha_1} s_t^{\alpha_2} N_t^{1-\alpha_1-\alpha_2} \quad (7)$$

where  $a_t$  is the total factor productivity (TFP), representing Hicks-neutral technological change, and where  $0 < \alpha_1, \alpha_2 < 1$ , are the elasticities of output with respect to Earth capital and space capital, respectively. Labor is assumed to be equal (or proportional) to population, and hence the labor growth rate is equal to the population growth rate.

The representative firm maximizes profits by choosing the appropriate levels of capital and satellites given population dynamics. Profits are defined as,

$$\pi_t = y_t - r_t^k k_t - r_t^s s_t - w_t N_t \quad (8)$$

3.1.3 *Launch cost* The installation cost function is defined as:

$$l_t = m_t i_t^s \quad (9)$$

where  $m_t$  is the fraction of launch costs over the total investment cost in space capital. The installation cost is assumed to represent only a fraction of the total investment cost. In the macroeconomic literature, investment adjustment costs are commonly used to smooth capital accumulation and to replicate observed investment dynamics. These costs reflect the idea that adjusting the capital stock is not frictionless, that is, firms cannot install or reallocate capital instantly or without cost. For space capital, this consideration is particularly important, as installation costs reduce the effective amount of new capital that can be accumulated from each unit of investment expenditure. Adjustment costs are typically modeled as convex functions, implying that the marginal cost of investment increases with the scale of adjustment. However, non-convex or fixed adjustment cost structures have also been proposed in the literature (see, for example, Lucas, 1967; Caballero and Engel, 1999; Christiano et al., 2005). In the case of space investment, though, launch costs do not exhibit these properties as they are effectively fixed costs, determined primarily by the satellite's mass and target orbit altitude, and are charged as a constant amount per kilogram. Therefore, the fraction of investment in space capital that accumulates into operational satellites is defined as,

$$h_t = (1 - m_t) i_t^s \quad (10)$$

It is assumed that  $m_t$  is a decreasing function of time, representing decreasing launch costs based on a learning curve. The launch cost at each period is given by,

$$m_{t+1} = \exp(g_{m,t}) m_t \quad (11)$$

$$g_{m,t} = g_{m,0} (\exp(-\delta_m t)) \quad (12)$$

where  $g_{m,0} < 0$  is the initial change in the launch cost.

3.1.4 *Exogenous growth sources* The model incorporates three exogenous sources of growth: aggregate neutral technological change, investment-specific technological change for satellites, and aggregate labor growth. The growth rates of technical change and population are not constant, but similarly to climate change IAMs it is assumed that the growth rate declines over time. Aggregate productivity technological progress is characterized as,

$$a_{t+1} = \exp(g_{a,t})a_t \quad (13)$$

where  $g_{a,t}$  is the growth rate of TFP defined as,

$$g_{a,t} = g_{a,0}\exp(-\delta_a t) \quad (14)$$

where  $\delta_a$  is the decay rate in the TFP growth rate, and  $g_{a,0}$  is the TFP growth rate at the initial period ( $t = 0$ ). We assume a similar specification for the satellite investment-specific technological progress,

$$q_{t+1} = \exp(g_{q,t})q_t \quad (15)$$

where  $g_{q,t}$  is the growth rate of ISTC defined as,

$$g_{q,t} = g_{q,0}\exp(-\delta_q t) \quad (16)$$

where  $\delta_q$  is the decay rate in ISTC for satellites, and  $g_{q,0}$  is ISTC growth rate at the initial period.

Finally, we define the dynamics of the population,  $N_t$ . Population is another source of growth as it is assumed that labor equals population. Following the specification by Hassell (1975), population dynamics is defined as,

$$N_{t+1} = N_t \left( \frac{N^*}{N_t} \right)^\zeta \quad (17)$$

where  $N^*$  is the asymptotic population at the end of the simulation period and  $\zeta$  is a parameter driving the population growth rate.

3.1.5 *Economic to physical variables mapping* Space environment is defined by physical variables. Some of these variables have an economic counterpart but no others. On the other hand, some physical variables resulted from economic decisions are key for the dynamics of orbital debris. In order to ensure that economic and physical variables are integrated correctly, a mapping between the economy and the space must be established. On the other hands, We use the number of new satellites inserted into orbit as the numerary for this mapping.

The first step in the economic-physical variables mapping consists in assuming that the relationship between investment in satellites net of launch costs,  $h_t$ , and the number of new satellites inserted into orbit,  $H_t$ , is given by,

$$H_t = \mu h_t \quad (18)$$

where the parameter  $\mu$  represent a conversion parameter that transforms "economic" values into "physical" values.<sup>5</sup> Notice that this mapping means that satellite's ISTC affects the productivity value of the asset but not the quantity of assets. ISTC is considered as an embodied technological progress in new vintages of satellites. The higher the value of  $q_t$ , the larger the output-value of new satellites per unit of investment. In practice, a positive trend in  $q_t$  would reflect the decreasing manufacturing costs of satellites.<sup>6</sup> The second step in creating this mapping involves connecting the stock of satellites as a capital asset to output units,  $s_t$ , with the number of satellites,  $S_t$ , is given by,

$$S_t = \mu \frac{s_t}{q_t} \quad (19)$$

Similarly the number of satellites destroyed by collisions,  $X_t$ , is calculated as

$$X_t = \mu \frac{x_t}{q_t} \quad (20)$$

By substituting the above mappings into the restriction (6), we can derive the equivalent accumulation process for the number of satellites. Therefore, the stock of satellites, represented by the number of representative satellites, can be expressed as,

$$S_{t+1} = (1 - \delta_s)S_t + H_t - X_t \quad (21)$$

where  $0 < \delta_s < 1$  is the depreciation rate of satellites, and  $X_t$  is the number of destroyed satellites by collision with debris. Satellites is an equipment asset in orbit. Therefore, each period, the amount  $\delta_s S_t$  of satellites becomes non-operational and hence, automatically considered dead intact objects. Satellites that are no longer useful but remain in orbit are classified as orbital debris if not removed.

**3.1.6 Launches** The value of launches is just a fraction of investment in space capital in the economic part of the model but the number of launches plays a key role in the physical part. First, it is important to define the number of launches as an additional variable, given that the primary source of debris emission is the launching activity. Standard launch systems imply the use of rockets with several (two to four) stages. Some of these stages (parts of the launch vehicle, including fuel deposits and engines) remain in orbit one the payload has been inserted in orbit. Moreover, during the insertion phase, additional debris are generated as protection parts (i.e., fairings). Second, the number of launches is not equal to the number of satellites inserted into orbit. Indeed, the number of satellites per

<sup>5</sup>The parameter  $\mu$  can be interpreted as the (inverse) average monetary cost of a satellite. The variable  $h_t$ , the money spent in satellites, is defined in trillions of international 2023 dollars, whereas  $H_t$  is measured in units. Therefore, the average cost of each satellite is  $1/\mu$ . This fraction can be interpreted as the hedonic price of satellites, which is assumed to be constant over time for the technological characteristics of a representative satellite manufactured in the year 2023. The price of a satellite is then the ratio  $q_t/\mu$ , which is increasing over time reflecting embodied technological change.

<sup>6</sup>Notice that this assumption implies that ISTC does not affect the quantity of satellites, but each satellite is more productive. Alternatively, we could define the number of satellites inserted into orbit as  $H_t = \mu q_t h_t$ , where the number of new satellites depends on the ISTC, and hence,  $S_t = \mu s_t$ , and  $X_t = \mu x_t$ . However, we consider this alternative of little relevance, as this would imply no embodied technological change.

launch has been dramatically increases during the last decade. The availability of more powerful launches vehicles with higher payloads, together with the reduction in the size and weight of satellites has increased the number of satellites per launch. Therefore, the number of satellites inserted into orbit,  $H_t$ , is assumed to be a proportion  $\eta$  of the number of launches,  $L_t$ :

$$H_t = \eta L_t \quad (22)$$

and therefore, the parameter  $\eta$  can be interpreted as the the number of satellites per launch. Combining expressions (10), (18) and (22), we obtain the relationship between investment in space capital and the number of launches, given by,

$$L_t = \frac{\mu(1 - m_t)}{\eta} i_t^s \quad (23)$$

### 3.2 The space model

The space environment is vastly different from that of Earth. Space pollution can be either natural or man-made and can take the form of objects moving at high speeds that have the potential to collide with and destroy other objects. Any human-made object that is not functional and is orbiting around Earth is considered space junk. We will only consider man-made space debris since natural space pollution is rare and poses little threat to humans except in cases where a relatively large object is headed toward Earth. The Earth's atmosphere works as a protective shield against smaller objects that collide with our planet. Therefore, any damage resulting from such collisions remains confined to space. Here, we describe the physical space model incorporated into DISE-2024. This space-environmental module includes four main functions: the damage function, and three laws of motion for three types of orbital debris.

**3.2.1 The stock of pollution** The stock of orbital debris consists of all non-operational, human-made objects in orbit, excluding functional satellites and other active spacecraft. However, not all orbital debris are incorporated into the damage function. Prior to the first launch in 1957, the stock of orbital debris was zero, as humans had not yet ventured into space. Debris are highly heterogeneous in size, mass, and composition. Following the standard classification by ESA, we distinguish three categories for fragments: Fragments larger than 10 cm ( $F_{1,t}$ ), fragments between 1 cm and 10 cm ( $F_{2,t}$ ), and fragments between 1 mm and 1 cm ( $F_{3,t}$ ). Orbital debris is measured as the number of non-functional objects in orbit with a size greater than 1 cm.<sup>7</sup> The stock of debris as a function of their size,  $D_{i,t}$ , can be defined as,

$$D_{i,t} = W_t + Z_t + F_{i,t} \quad \text{for} \quad i = 1, 2, 3 \quad (24)$$

<sup>7</sup>The destruction power of debris smaller than 1 cm is estimated to be low and non-fatal in the case of a collision with a representative satellite, although they can cause serious damage in critical systems, reducing functionality and lifespan, and even disable small satellites. However, debris larger than 1 cm is potentially deadly due to the high velocity of the impact. Therefore, for computing the risk of collision and the damages, we consider the estimated number of pieces of debris larger than 1 cm.

where we distinguish three types of debris:  $W_t$  is the stock of derelict satellites abandoned in orbit,  $Z_t$  is the number of last stages rocket bodies, and  $F_{i,t}$  are fragments of size  $i$ . The key distinction is that fragments are dead debris, but both derelict satellites and rocket bodies are intact objects that can breakup, generating a large number of fragments, and can fragment in case of collision with each other or with other objects.

**3.2.2 Damage** Space pollution can cause a range of damages. Orbital debris poses a significant risk of collision with operational satellites and other spacecraft, leading to the loss of valuable equipment and the generation of even more debris. Although it is possible for uncontrolled large debris in low Earth orbit to re-enter the atmosphere and cause harm to life or property on the ground, the likelihood of such events is very low. However, orbital debris significantly increases operational costs for spacefaring entities.

The literature offers several alternative methods for calculating the probability of collision in space. Most approaches are based on the work of Farinella and Cordelli (1991), where the probability of collision is modeled as a function of the population of operational satellites and orbital debris. According to their framework, the number of satellites destroyed each period due to collisions with debris is assumed to depend on the amount of debris, the number of operational satellites, and the effectiveness of collision avoidance technologies,

$$X_t = (1 - v_t)\theta D_{2,t} S_t \quad (25)$$

where  $\theta > 0$  is a parameter representing the probability of collision,  $0 \leq v_t \leq 1$  is a variable representing successful avoidance collision maneuvers, and  $D_{2,t}$  is the population of orbital debris larger than 1 cm. If  $u_t$  takes the value of one, all possible collisions are avoided and no damage results from orbital debris. Notice that, given the above expression, the value of satellite assets destroyed by collision,  $x_t$ , is defined as,

$$x_t = (1 - v_t)\theta D_{2,t} s_t \quad (26)$$

When  $(1 - v_t)\theta D_{2,t} = 1$ , any space assets are destroyed rendering the space unusable. This point is reached when the pollution stock is  $D_{2,t} = 1/((1 - v_t)\theta)$ .

**3.2.3 Debris generation** Debris originates from various sources, including launch activities which generate derelict rocket upper stages and fuel tank remnants, and other mission related objects; derelict satellites that are not removed from orbit; accidental explosions and breakups; and the intentional creation of debris during military drills, such as destroying a satellite with an anti-satellite missile. The integrated model categorizes these into six main sources of orbital debris.

The first source of debris consists of mission-related objects (MRO), which are associated with the number of launches. This debris generation process is modeled as  $\omega L_t$ , where  $\omega$  represents the amount of debris created per launch during the launch period. This type of debris is classified as "fragments" and includes items such as protective fairings, covers, adapters, bolts, and cables. In addition to fragments, launches also generate another type of debris: the upper stages of launch vehicles, which often remain in orbit after deploying the payload. These rocket bodies constitute large intact debris with a

significant risk of breaking apart over time. The number of rocket bodies generated per launch is given by  $\varphi L_t$ , where  $0 \leq \varphi < 1$  represents the fraction of launches producing this type of debris. We assume that  $\varphi$  is strictly less than one, reflecting the existence of reusable launch vehicles and/or de-orbiting practices of upper stages once the payload has been inserted into orbit. Over time, these upper stages rocket bodies accumulate into a stock of debris, which will be formally defined later. The third source of debris consists of derelict satellites ( $W_t$ ). These are satellites that have reached the end of their operational lives, typically due to fuel depletion, and are abandoned in orbit rather than being de-orbited. Each period, the number of end-of-life satellites is represented by  $\delta_s S_t$ , where  $S_t$  is the total number of active satellites. Of these, a fraction  $0 \leq \chi \leq 1$  is abandoned in orbit each period, contributing to the stock of derelict satellites.

The fourth source of debris generation is fragmentation events, which occur due to explosions and breakups of both derelict satellites and rocket bodies. These events can be either unintentional or deliberate. Unintentional fragmentation debris arises from the breakup of operational satellites, rocket bodies, or engines. The primary cause of in-orbit explosions is the residual fuel left in the tanks of upper-stage rockets and satellites. In the harsh conditions of outer space, mechanical components and devices degrade quickly, leading to leaks that mix fuel components. This can trigger self-ignition, resulting in accidental explosions that destroy the source object and scatter its mass into countless fragments of varying sizes and velocities. Batteries can also explode.

The fifth source of debris is also in-orbit endogenously driving, and is the result of collision among both operational and non-operational objects. The model distinguishes two types of collisions: The collision between a piece of debris and an operational satellite, and the collision of intact debris (i.e., derelict satellites and upper stages rocket bodies) with each other and with fragments.

Finally, intentional fragmentation events, on the other hand, involve deliberate actions such as spacecraft interceptions using surface-launched missiles. These have been significant contributors to debris in recent years. Four countries, the United States, Russia, China, and India, have conducted direct-ascent anti-satellite (ASAT) tests, significantly increasing the population of orbital debris.

From these sources of emissions, we identify three equations describing the accumulation process for three types of orbital debris: Derelict satellites, rocket bodies and fragments. The two first types of debris are intact objects which are subject to fragmentation events. It is worth noting that the model considers two distinct processes for orbital debris generation. The first is tied to economic activity, specifically launches and the operational procedures of launch vehicles. The second is an endogenous process involving in-orbit emissions from breakups and collisions. The calibration of debris generation per launch recognizes that debris is not only created at the time of the launch but also in subsequent periods. This includes debris from rocket bodies, engines, and abandoned derelict satellites, which can generate additional fragments through breakups and explosions caused by residual fuel, and collisions.

**3.2.4 Derelict satellites** The stock of derelict satellites in orbit decreases due to natural decay, breakups, and collision with debris, and increases with end-life satellites abandoned

in orbit. Formally, the law of motion of derelict satellites is given by,

$$W_{t+1} = (1 - \delta_w)W_t - \varepsilon_w W_t - \theta(D_{2,t} + (1 - v_t)S_t)W_t + \chi\delta_s S_t \quad (27)$$

where  $\delta_w$  is the natural decay rate of derelict satellites due to atmospheric drag and solar conditions, and  $\varepsilon_w$  is the fraction of derelict satellites that breakup each period. The term  $\theta(D_{2,t} + S_t)W_t$  reflects the number of derelict satellites that are destroyed by collision with fragments, other derelict satellites, rocket bodies and operational satellites. The dynamics of the stock of abandoned end-life satellites into orbit would depend on the regulatory policies about end-mission disposal. In case of explosion, it is assumed that the number of debris generated is  $\phi_z \varepsilon_w W_t$ , where  $\phi_z$  is the number of fragments resulting from the breakup. The number of debris produced by collisions of a derelict satellite with any other object is  $\gamma_w \theta(D_{2,t} + (1 - v_t)S_t)W_t$ .

**3.2.5 Rocket bodies** The accumulation process for rocket bodies is similar. The law of motion for the stock of upper stage body rockets is defined as,

$$Z_{t+1} = (1 - \delta_z)Z_t - \varepsilon_z Z_t - \theta(D_{2,t} + (1 - v_t)S_t)Z_t + \varphi L_t \quad (28)$$

where  $\delta_z$  is the natural decay rate of rocket bodies, and  $\varepsilon_z$  is the fraction of body rockets that breakup each period. The number of debris produced by rocket bodies breakups is  $\phi_z \varepsilon_z Z_t$ , where  $\phi_z$  is the amount of debris produced by the breakup of a body rocket. The number of debris produced by collisions of a rocket bodies with any other type of object is  $\gamma_z \theta(D_{2,t} + (1 - v_t)S_t)Z_t$ .

**3.2.6 Fragments** Finally, the third type of debris considered are fragments. The stock of fragments increases depending on the number of launches, fragments from breakups of derelict satellites and body rockets, and collisions between debris and operational satellites. We assume that the law of motion of fragments larger than 10 cm is given by,<sup>8</sup>

$$F_{1,t+1} = (1 - \delta_f)F_{1,t} + \omega L_t + \gamma_s X_t + \phi_w \varepsilon_w W_t + \phi_z \varepsilon_z Z_t + \gamma_w \theta D_{2,t} W_t + \gamma_z \theta D_{2,t} Z_t \quad (29)$$

where  $\delta_f$  is the natural decay of debris fragments,  $\omega$  is the amount of debris produced per launch (MRO), and  $\gamma_s$  is the amount of debris created by a collision and destruction of operational satellites. The parameter  $\gamma_w$  is the number of fragments from the collision of derelict satellites, and  $\gamma_z$  is the number of fragments from collision of rocket bodies. The model excludes the possibility that operational satellites can breakup due to design failures, and fragments resulting from military anti-satellite (ASAT) tests with direct-ascent missiles.

<sup>8</sup>The model computes the population of fragments ( $F_{1,t}$ ) and debris larger than 10 cm ( $D_{1,t}$ ) for two reasons. First, there is a computational reason for limiting the scale of this variable. Second, most parameters are calibrated using data about cataloged objects in orbit, which usually include only objects larger than 10 cm. From that we obtain the population of debris larger than 1 cm ( $D_{2,t}$ ) using a scale parameter based on the estimation of debris between 1 cm and 10 cm from the ESA.

### 3.3 Finite-horizon conditions

The growth model assumes an economy populated by forward-looking agents with rational expectations who make decisions over an infinite horizon. However, in practice, numerical solutions can only be computed over a finite number of periods. This requires transforming the original infinite-horizon optimal control problem into an equivalent finite-horizon version. A key challenge in this transformation is determining the appropriate terminal condition, particularly the level of capital stock in the final period of the finite-horizon solution. The choice of this terminal condition critically affects the accuracy of the approximation to the true infinite-horizon equilibrium. As noted by Mercenier and Michel (1994), solving nonlinear infinite-horizon optimization problems—especially in continuous time—requires reformulating the problem as a finite-horizon discrete-time approximation. This reformulation involves three main decisions: (1) selecting the length of the planning horizon, (2) determining how to account for behavior beyond the terminal period, and (3) choosing the sequence and frequency of time intervals in the discretization. If the finite horizon is too short or the terminal condition is poorly chosen, the resulting solution path may deviate significantly from the true infinite-horizon trajectory. These issues can be mitigated either by extending the planning horizon, at the cost of greater computational complexity, or by reducing the frequency of the time intervals, thereby lowering the number of decision points to solve.

The general infinity-horizon problem can be defined as an utility maximization problem which is divided in two parts,

$$\max_{c_t} W = \sum_{t=0}^T \left( \frac{1}{1+\rho} \right)^t U(c_t) + \sum_{t=T+1}^{\infty} \left( \frac{1}{1+\rho} \right)^t U(c_t) \quad (30)$$

where the first part is the finite-horizon already solved from  $t = 0$  to  $T$ , and the second part represents the economy behavior from period  $T + 1$  to infinity, and where the two sub-problems are linked through the capital stock at period  $T + 1$ .

The literature has dealt with this issue proposing alternative terminal conditions to be incorporated into the model to determine investment in the last computational period ( $T$ ) but using some adjustment to approximate choices over the period  $T + 1$  to infinity. The simplest approach is to assume that the world ends at period  $T$ . This can be a valid method when the value of  $T$  is large and the discount rate is high just to minimize the effects of the terminal values on the optimal path. Because  $\beta^t \rightarrow 0$  as  $t \rightarrow \infty$ , we can truncate the infinite horizon at a large finite period  $T$ . Other approaches assume that the economy reaches its steady state at time  $T$ . Blake and Westaway (1995) argue that any distortionary effects of a terminal condition can be minimized by setting a terminal condition consistent with the steady state of the model and sufficiently distant so that it does not affect model properties over the horizon of interest, so that a change either in the horizon period or in the terminal condition does not alter the solution over the period of interest.<sup>9</sup>

<sup>9</sup>During the 1960s, this issue has been extensively studied by the literature of economic planning, where alternative strategies for dealing with the terminal condition have been proposed. Frisch (1955) proposes the use of geometric growth terminal conditions for numerical planning problems. Chakravarty (1962) considers

An alternative frequently used in climate-change economics is to use a fixed saving rate for the last periods of the simulation together with the use of large time intervals. This is the strategy followed by, for instance, Nordhaus (1992, 1993) in solving the DICE model. For instance, in DICE-2016 (Nordhaus, 2017) it is used a constant saving rate equal to the long-run saving rate for the last 10 periods (50 years). In DICE-2023 (Nordhaus, 2024) it is used a saving rate of 0.28 for periods larger than 37 (last 185 years). using an alternative approach, Nordhaus (2008) assumes that investment at the terminal time must be at least 2% of the capital stock at the terminal time. Cai et al. (2012) also solve the DICE model and assume that at the terminal time, the world reaches a partial equilibrium. They solve the model for a horizon of 600 years and estimate utility for a further 800 years using complete Chebyshev polynomial over the states.

Barr and Manne (1967) assume that at the terminal period  $T$ , the economy is at the steady state where the growth rate is  $g_y$ . Under these assumption, expression (30) can be written as,

$$\max_{c_t} W = \sum_{t=0}^{T-1} \left( \frac{1}{1+\rho} \right)^t U(c_t) + \sum_{t=T}^{\infty} \left( \frac{1}{1+\rho} \right)^t U(c_t(1+g_y^{t-T})) \quad (31)$$

where the second term is a constant. Abstracting from the constant term, the maximization problem can be written as,

$$\max_{c_t} W = \sum_{t=0}^{T-1} \left( \frac{1}{1+\rho} \right)^t U(c_t) + \frac{1+\rho}{\rho(1+\rho)^T} U(c_T) \quad (32)$$

$$\max_{c_t} W = \sum_{t=0}^T \hat{\beta}^t U(c_t) \quad (33)$$

where the discount factor would be,

$$\hat{\beta}^t = \begin{cases} \left( \frac{1}{1+\rho} \right)^t & \text{for } t < T \\ \frac{(1+\rho)^{1-T}}{\rho} & \text{for } t = T \end{cases} \quad (34)$$

At the terminal period, gross investment is determined by the size of capital stock in the terminal period, the exogenous growth rate (all quantities growth at the same rate in the steady state), and the capital depreciation rate. The constraint of investment would be,

$$i_T = (g_y + \delta)k_T \quad (35)$$

This is the strategy we follow for the baseline solution of the model, by combining the discount factor given by expression (34), with the following two investment constraints

---

that terminal capital stock is given by a proportion relative to the initial capital stock which implies that capital stock grows at some exogenous rate. Stoleru (1965) introduces the terminal condition that capital stock growth rate after  $T$  equals the exogenous rate of labor force (i.e., population). Manne (1970) formulates sufficient conditions for any planning problem to provide a solution which is not only optimal for a horizon  $T$ , but is also optimal for all finite horizon greater than  $T$ .

for Earth and space capital, respectively,

$$i_T \geq (g_y + \delta_k)k_T \quad (36)$$

and

$$h_T \geq \frac{(g_y + \delta_s)s_T}{q_T} \quad (37)$$

#### 4. COMPETITIVE DECENTRALIZED EQUILIBRIUM

This section compute the first order conditions for the decentralized solution using the Lagrangian auxiliary function. The resulting differential equation systems will be later approximated numerically as a nonlinear programming problem.

The household maximization problem, taking into account the accumulation process for both capital and satellites, is given by,

$$\begin{aligned} \mathcal{L} = E_0 \sum_{t=0}^{\infty} \beta^t U(\hat{c}_t) N_t \\ - \sum_{t=0}^{\infty} \lambda_t [c_t + k_{t+1} - (1 - \delta_k)k_t + \frac{1}{q_t(1 - m_t)} [s_{t+1} - (1 - \delta_s)s_t + (1 - v_t)\theta \bar{D}_{2,t} s_t \\ - r_t^k k_t - r_t^s s_t - w_t N_t - \pi_t] \end{aligned} \quad (38)$$

where  $\bar{D}_{2,t}$  is the exogenous amount of orbital debris. Hence, orbital debris affects the optimal decision by the agent but their social costs are not internalized.

First order conditions from  $t = 0, 1, \dots, \infty$ , are:

$$\frac{\partial \mathcal{L}}{\partial c_t} = \beta^t U'_c(c_t) - \lambda_t = 0 \quad (39)$$

$$\frac{\partial \mathcal{L}}{\partial k_{t+1}} = -\lambda_t + \lambda_{t+1}(1 - \delta_k + r_{t+1}^k) \quad (40)$$

$$\frac{\partial \mathcal{L}}{\partial s_{t+1}} = \frac{\lambda_t}{q_t(1 - m_t)} - \frac{\lambda_{t+1}}{q_{t+1}(1 - m_{t+1})} [1 - \delta_s - (1 - v_t)\theta \bar{D}_{2,t+1}] + \lambda_{t+1} r_{t+1}^s = 0 \quad (41)$$

From the maximization problem, solving for the Lagrangian's multiplier, equilibrium conditions are given by,

$$U'_c(c_t) = \beta E_t U'_c(c_{t+1}) [1 - \delta_k + r_{t+1}^k] \quad (42)$$

$$U'_c(c_t) = q_t(1 - m_t) \beta E_t U'_c(c_{t+1}) \left[ \frac{1 - \delta_s - (1 - v_t)\theta \bar{D}_{2,t+1}}{q_{t+1}(1 - m_{t+1})} + r_{t+1}^s \right] \quad (43)$$

Expression (42) is the standard Euler equation for optimal investment decisions in capital excluding satellites. Expression (43) is also an Euler equation, but it pertains to

the investment decision in satellites, where the cost of destruction by collision is incorporated. The term  $\theta\bar{D}_{t+1}$  accounts for the sudden, full depreciation of satellites stock due to collisions. As the quantity of orbital debris increases, the rental price of satellite to capital also increases.

From the profit maximization problem of the representative firm we have:

$$r_t^k = a_t f'_k(k_t, s_t, N_t) \quad (44)$$

$$r_t^s = a_t f'_s(k_t, s_t, N_t) \quad (45)$$

$$w_t^s = a_t f'_N(k_t, s_t, N_t) \quad (46)$$

Equilibrium conditions are obtained by substituting (44) and (45) into (42) and (43),

$$U'_c(c_t) = \beta E_t U'_c(c_{t+1}) [1 - \delta_k + a_{t+1} f'_k(k_{t+1}, s_{t+1})] \quad (47)$$

$$U'_c(c_t) = q_t (1 - m_t) \beta E_t U'_c(c_{t+1}) \left[ \frac{1 - \delta_s - (1 - v_t) \theta \bar{D}_{2,t+1}}{q_{t+1} (1 - m_{t+1})} + a_{t+1} f'_s(k_{t+1}, s_{t+1}) \right] \quad (48)$$

Equating both expressions we find that the arbitrage condition for investing in both Earth and space capital is,

$$[1 - \delta_k + a_{t+1} f'_k(k_{t+1}, s_{t+1})] = q_t (1 - m_t) \left[ \frac{1 - \delta_s - (1 - v_t) \theta \bar{D}_{2,t+1}}{q_{t+1} (1 - m_{t+1})} + a_{t+1} f'_s(k_{t+1}, s_{t+1}) \right] \quad (49)$$

## 5. DECENTRALIZED SOLUTION APPROACH

The core idea of our approach builds on the fixed-point iteration method proposed by Krusell and Smith (2024) in the context of climate change. In their framework, the competitive equilibrium is computed by iterating on agents' expectations about aggregate environmental and economic variables. Specifically, they begin with an initial guess for the trajectory of global temperature and the sequence of interregional transfers (e.g., carbon tax revenues). Given these, they solve the Bellman equation backward in time to derive time-dependent policy functions (decision rules) for households and firms. These policy functions are then used to simulate the economy forward, generating updated paths for aggregate capital, consumption, emissions, and temperature. The iteration continues until the guessed and simulated trajectories converge, forming a fixed point that is consistent with a decentralized equilibrium in which agents do not internalize externalities.

In this paper, we adopt a conceptually similar approach but adapt it to the context of orbital environmental externalities, using a nonlinear programming (NLP) formulation instead of dynamic programming. Rather than computing policy functions, we solve a finite-horizon dynamic optimization problem directly at each iteration using numerical optimization tools. The model represents a decentralized economy in which agents maximize utility and profits based on private returns, taking the trajectory of orbital debris and associated damages as exogenous.

The fixed-point pseudo-algorithm is given in Algorithm 1.

---

**Algorithm 1** DISE-2024D (Competitive Decentralized Equilibrium)

---

**Initialize:** Set initial conditions and guess for debris paths ( $W(t), Z(t), F(t)$ , etc.)

**Main Iteration Loop:**

**for** iter = 1 to max\_iter **do**

    Solve the NLP optimization problem: maximize total discounted utility

    Update orbital debris dynamics

    Propagate state to  $t + 1$

    Update damage

    Compute difference between updated and previous satellites destroyed  $X_t$

**if** converged (difference < tolerance) **then**

**Break**

**end if**

**end for**

**Output:** Optimal path for economic variables and orbital debris for a decentralized setting

---

The fixed-point algorithm proceeds as follows:

1. **Initialization:** Start with an initial guess for the time paths of the externality, specifically, the trajectory of orbital debris  $\{W_t, Z_t, F_t\}$ , and the associated damages  $\{X_t\}$  over a finite horizon  $t = 0, 1, 2, \dots, T$ .
2. **Optimization Step:** Given the externality paths  $\{W_t, Z_t, F_t, X_t\}_{t=0}^T$ , solve the decentralized economic model of previous section as a nonlinear programming problem. The decision variables include consumption, Earth capital investment, space capital investment and satellite deployment, subject to economic constraints (capital accumulation, resource constraints) and environmental constraints (e.g., satellite destroyed due to debris collisions). Since agents do not internalize debris-related damages, the externality affects the economy only through its impact on the stock of operational satellites.
3. **Forward Simulation:** Using the optimal trajectories of economic activity computed in previous step (e.g., satellite launches), compute the resulting updated path of debris and damage using the debris accumulation equations and the damage function (collision probabilities, emissions, fragmentation dynamics, and natural decay processes).
4. **Fixed-Point Update:** Compare the updated debris and damage trajectories to the previous iteration. If the difference is below a specified convergence tolerance (e.g., based on a norm of the difference between successive  $X_t$  paths), stop. Otherwise, update the externality path and return to Step 2.

This iterative process continues until convergence is achieved, yielding a self-consistent equilibrium trajectory in which the economic decisions are optimal given the assumed externality, and the externality evolves endogenously based on those decisions. This approach provides a rigorous method for computing the BaU scenario in a decentralized economy with environmental feedbacks, without requiring agents to internalize, even a small fraction, the externality.

## 6. DATA AND CALIBRATION

To compute the model numerically, we require initial values for the state and exogenous variables, with the simulation starting in the year 2023, as well as a calibration of the economic and space-related parameters. A detailed description of the model's calibration is provided in the online appendix.

## 7. RESULTS

This section presents the main results from the simulation of the model for a competitive decentralized economy, where both households and firms take optimal decisions without internalizing the externality, and for a centralized economy, where the objective is to maximize social welfare and the externality is fully internalized. To perform the numerical simulations, the model is reformulated as a non-linear programming (NLP) problem. The simulations cover the period from 2023 to 2152, providing a planning horizon of 150 years, with results generated at an annual frequency. The fixed point algorithm for a decentralized solution is implemented in GAMS and the model solved with the CONOPT4 algorithm.

The trajectories for the decentralized economy are compared with the first-best trajectories of a social planner. In the former scenario, there is no authority, national or international, who take actions to slowdown the growth of orbital debris or to internalize the orbital debris externality. Spacefaring agents simply adapt to the space environment and take the amount of debris as given. This fairly represents the current scenario, where no active action is taken to mitigate orbital debris. The starting point is the number of debris existing in the year 2023. This baseline scenario represents an environment where the current policy is maintained without changes in the future. The consideration of outer space as an international common resource and the difficulties for an international agreement to mitigate debris generation and reduce the stock of orbital debris give this scenario a high probability. In this baseline scenario households and firms take as given the stock of orbital debris, with no internalization of the externality by any authority.

The second scenario represent the first-best with no specific debris mitigation policy. In this scenario there is a central planner that maximize social welfare, but no direct instrument to mitigate orbital debris is available. This means that no debris mitigation policy is used and no mandatory debris mitigation guideline is enforced. Nevertheless, in this scenario the social planner fully internalize the orbital debris externality by choosing the optimal investment in Earth and space capital. This means that trajectories of the variables are optimal given the effect of the economy on the space environment. Climate-change literature usually identifies this scenario with the BAU (business-as-usual) case. Nordhaus

(2008) interprets this scenario as a situation in which households and firms adapt to the environment but governments take no action to mitigate emissions or to internalize the environmental negative externality. However, as shown by Shiell and Lyssenko (2008) this is a social optimum solution in which the externality is fully internalized, even without policy instruments.

Figure 1 plots the trajectories of orbital debris over time. As expected, we observe the characteristic "hockey-stick" shape in both total debris and fragments, driven by the endogenous in-orbit creation of debris (see Bongers and Torres, 2025). Both derelict satellites and rocket bodies exhibit tipping-point behavior. The figure compares the decentralized *laissez-faire* scenario with the first-best (central planner) solution. As anticipated, the *laissez-faire* scenario leads to a significantly more polluted orbital environment. Although the trajectories are nearly indistinguishable in the early years, the decentralized path consistently results in a higher accumulation of debris throughout the simulation horizon. The key result is that debris accumulation accelerates significantly toward the end of the

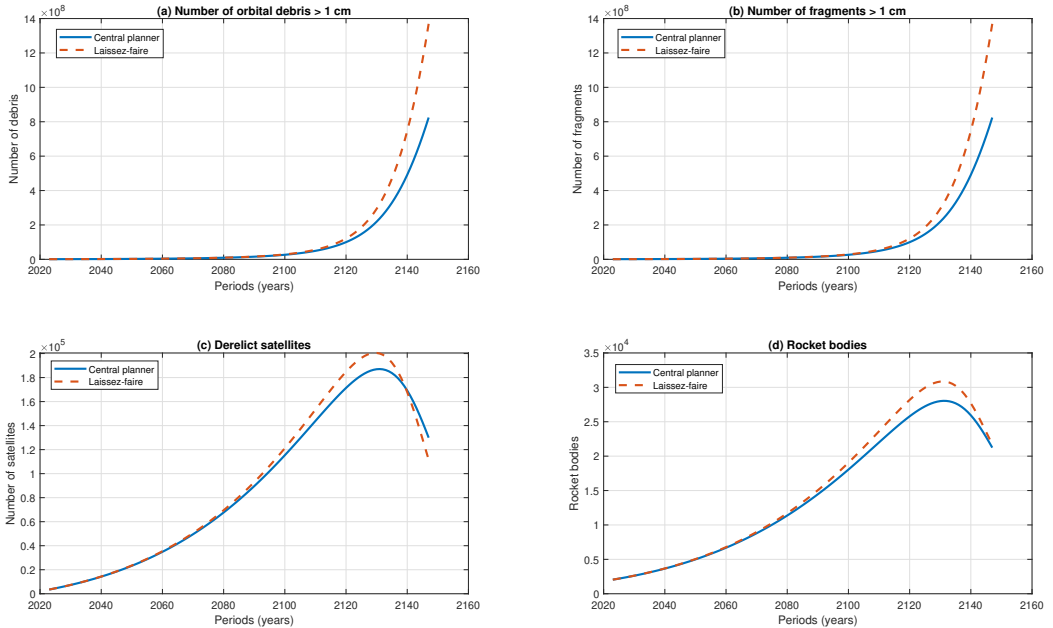


FIGURE 1. Paths for orbital debris.

This figure shows the trajectories for orbital debris. Panel (a) shows total orbital debris larger than 1 cm. Panel (b) shows the number of fragments larger than 1 cm. Panel (c) shows the stock of derelict satellites abandoned in orbit. Panel (d) shows the stock of upper stages rocket bodies that are not deorbited and remains in Earth's orbit. Total orbital debris is the sum of fragments, derelict satellites and rocket bodies. Solid lines represent the central planner solution. Dash lines represent the competitive decentralized solution.

period under the decentralized scenario due to the feedback loop from endogenous debris generation. Derelict satellites and rocket bodies both accumulate at a faster rate in the decentralized setting, following a hump-shaped trajectory. However, the larger debris population also leads to a higher collision rate, which in turn reduces the stock of intact objects. Eventually, this dynamic results in a crossover point where the number of intact objects in the centralized economy exceeds that in the decentralized one.

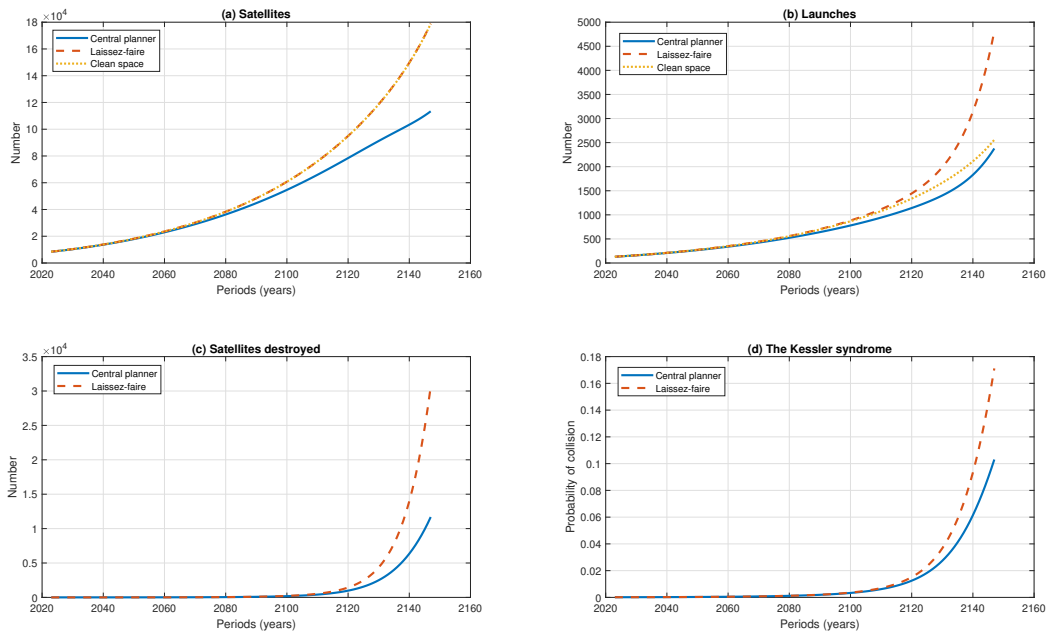


FIGURE 2. Number of operational satellites, launches, operational satellites destroyed by collisions, and the probability of collision of operational satellites.

This figure shows the optimal trajectories for the number of satellites (panel a), number of launches (panel b), number of satellites destroyed by collisions (panel c), and the probability of collision (panel d). Solid lines represent the central planner solution. Dash lines represent the competitive decentralized solution. Panels (a) and (b) also show the number of satellites and number of launches for an scenario with no debris (dotted lines).

Figure 2 presents the trajectories for four key indicators: the number of operational satellites, the number of launches, the number of satellites destroyed by collisions, and the probability of collision, which serves as a proxy for the onset of the Kessler syndrome. For both satellites and launches, the figure also includes a benchmark scenario representing a clean orbital environment with no debris externality. In the case of operational satellites, we find that the trajectory under the *laissez-faire* scenario closely resembles the one without any debris externality. This suggests that, at least over the simulated horizon, the damages

from debris are relatively limited, and the behavioral response of agents remains modest in the presence of the externality. In contrast, the centralized (first-best) solution displays a more conservative trajectory, with a lower stock of satellites, reflecting the internalization of long-term environmental costs by the social planner.

The trajectory for launches shows a slightly different pattern. Under the *laissez-faire* scenario, the number of launches is significantly higher than in the clean-space benchmark. This is primarily because some satellites are destroyed by collisions and must be replaced, leading to a sustained increase in launch activity. In contrast, the launch trajectory in the clean environment closely resembles that of the centralized (first-best) scenario. However, the centralized scenario results in fewer launches than even the clean-space case, as the planner fully internalizes the negative externality. This internalization leads to a more cautious deployment of satellites and, consequently, a lower number of launches overall.

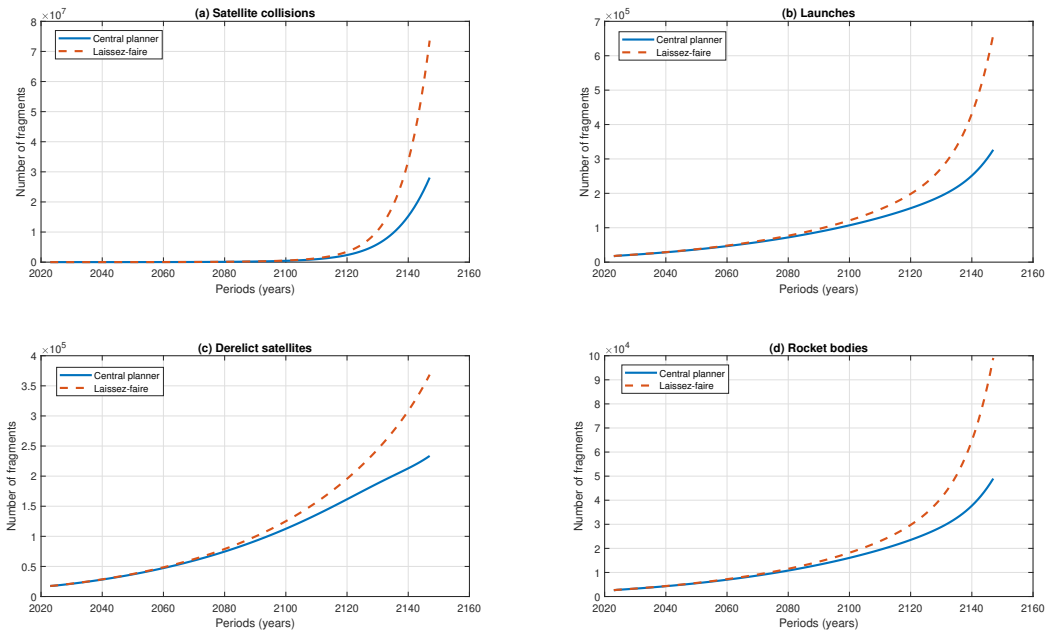


FIGURE 3. Sources of emissions of orbital debris (I): Collisions of operational satellites, fragments from launches, and number of intact objects.

This figure shows the trajectories for debris emissions. The figure plots four sources of emissions. Panel (a) shows debris emissions by collisions of operational satellites. Panel (b) shows debris emissions from launches. Panel (c) shows debris emission from derelict satellites abandoned in orbit. Panel (d) shows debris emissions from rocket bodies abandoned in orbit. Solid lines represent the central planner solution. Dash lines represent the competitive decentralized solution.

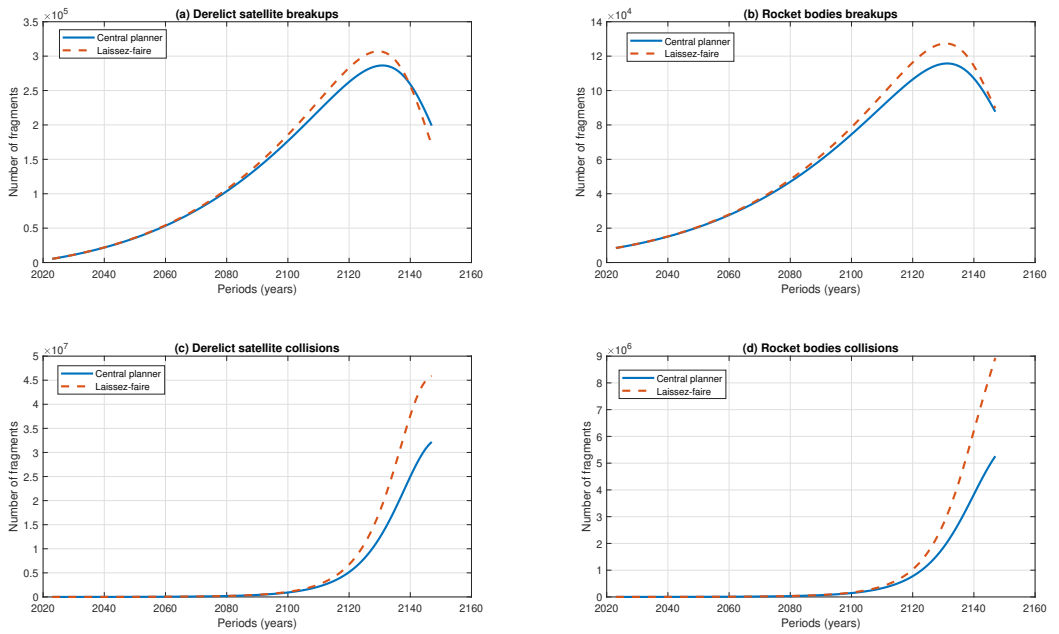


FIGURE 4. Sources of emissions of orbital debris (II): Debris breakups and collisions.

This figure shows the trajectories for debris emissions. The figure plots four sources of emissions. Panel (a) shows debris emissions from the breakup of derelict satellites. Panel (b) shows debris emissions from the breakup of rocket bodies. Panel (c) shows debris emission from derelict satellites collisions. Panel (d) shows debris emissions from rocket bodies collisions. Solid lines represent the central planner solution. Dash lines represent the competitive decentralized solution.

Panel (c) shows the number of satellites destroyed by collisions with orbital debris. The difference between the two scenarios reflects both the varying accumulation of debris and the differing stock of satellites. As in previous figures, we observe a characteristic upward "hockey-stick" shape, particularly under the *laissez-faire* scenario. Panel (d) presents the probability of collision for operational satellites. Over the simulation horizon, this probability rises steadily, reaching approximately 20% in the *laissez-faire* scenario and just over 10% in the centralized (first-best) case. The steeper trajectory under *laissez-faire* indicates that, if current trends continue, the probability of collision would approach 100% within just a few additional years, signaling a tipping point toward runaway debris accumulation and potential loss of orbital viability.

Figures 3 and 4 plot the path for emissions. The model account for eight different sources of debris fragments emissions: Launches, derelict satellites, rocket bodies, derelict satellites breakups, rocket bodies breakups, operational satellites collisions, derelict satellites collisions, and rocket bodies collisions. In the long-run, the main source of debris

emission is collision, principally, collisions of operational satellites. In all the cases, debris emission are larger under *laissez-faire* compared to a centralized scenario. The second source of debris fragments emission is derelict satellites collision, followed by rocket bodies collisions, launches, and derelict satellites breakups.

## 8. CONCLUSIONS

This paper presents a fixed-point approach for solving Integrated Assessment Models (IAMs) in a competitive decentralized economy with environmental externalities. The competitive decentralized equilibrium is often referred to as the Business-as-Usual (BaU) scenario or *laissez-faire*. However, there is considerable confusion in the literature regarding the interpretation of this solution. It is frequently mistaken for a central planner's solution in which no emission mitigation policy is implemented. This confusion arises because the solution for a central planner's problem is straightforward, it can be obtained directly by solving a numerical nonlinear programming (NLP) problem, whereas solving for the decentralized equilibrium is a more complex task. This is particularly true in the case of Nordhaus' DISE model, arguably the most widely used climate-change IAM, where the BaU scenario is often mistakenly identified with a central planner who maximizes social welfare without imposing any abatement policy.

In this paper, we use a similar approach to Krusell and Smith (2024) to obtain the decentralized solution for the DISE-2024 model. The algorithm solves the problem of maximization of households and firms given an initial exogenous path for orbital debris. Then, the path for orbital debris and the risk of collision are updated given the optimal decisions by households and firms, and a new maximization takes place in an iterative process, until convergence.

We find that the decentralized solution produces more orbital debris and more launch activity compared to a first-best central planner solution with no abatement policy, as agents do not internalize the social cost of the externality. The comparison between both solutions establishes a benchmark for the design and implementation of debris mitigation policies and is a measure of the social cost of orbital debris. We also compare the trajectory for operational satellites with a sci-fi scenario representing a clean space without orbital debris. We find that the trajectory under the clean scenario is very close to the trajectory of the *laissez-faire*, indicating that destroyed satellites are replaced in the BaU scenario.

## REFERENCES

- [1] Barr, J. R. and Manne, A. S. (1967). Numerical experiments with finite horizon planning models. *Indian Economic Review*, 2(1): 1-29.
- [2] Blake, A. P. and Westaway, P. F. (1995). An analysis of the impact of finite horizons on macroeconomic control. *Oxford Economic Papers*, 47(1): 98-116.
- [3] Bongers, A. and Torres, J. L. (2023). Orbital debris and the market for satellites. *Ecological Economics*, 209: 107831.
- [4] Bongers, A. and Torres, J. L. (2024). Star Wars: Anti-Satellite weapons and orbital debris. *Defence and Peace Economics*, 35(7): 826-845.

- [5] Bongers, A. and Torres, J. L. (2025). Optimal path for orbital debris. SEWP-06-2025.
- [6] Bongers, A., Molinari, B., Rouillon, S. and Torres, J. L. (2024). The foundations of the economics of the outer space: A premier overview. SEWP-01-2024, Institute for Space Economics.
- [7] Bongers, A., Ortiz, C. and Torres, J.L. (2025). DISE: A dynamic integrated space economy model for orbital debris mitigation policy evaluation. *Environmental and Resource Economics*, 88(8): 2125-2156.
- [8] Caballero, R. J. and Engel, E. M. R. A. (1999). Explaining investment dynamics in U.S. manufacturing: A generalized (S,s) approach. *Econometrica*, 67(4): 783-826.
- [9] Cass, D. (1965). Optimal growth in an aggregative model of capital accumulation. *Review of Economic Studies*, 32: 233-240.
- [10] Chakravarty, S. (1962). The Existence of an Optimum Savings Program. *Econometrica*, 30(1): 178-187.
- [11] Christiano, L., Eichebaum, M. and Evans, C. (2005). Nominal rigidities and the dynamics effects of a shock to monetary policy. *Journal of Political Economy*, 113: 1-45.
- [12] Golosov, M., Hassler, J., Krusell, P. and Tsyvinski, A. (2014). Optimal taxes on fossil fuel in general equilibrium. *Econometrica*, 82(1): 41-88.
- [13] Greenwood, J., Hercowitz, Z. and Krusell, P. (1997). Long-Run Implications of Investment-Specific Technological Change. *American Economic Review*, 87(3): 342-362.
- [14] Hassell, M. P. (1975). Density-dependence in single-species populations. *British Ecological Society*, 44(1): 283-295.
- [15] Hassler, J. and Krusell, P. (2012). Economics and climate change: Integrated assessment in a multi-region world. *Journal of the European Economic Association*, 10(5): 974-1000.
- [16] Hassler, J., Krusell, P. and Olovsson, C. (2021). Suboptimal climate policy. *Journal of the European Economic Association*, 19(6): 2895-2928.
- [17] Kessler, D. J. (1991). Collisional cascading: The limits of population growth in low earth orbit. *Advances in Space Research*, 11(12): 63-66.
- [18] Kessler, D. J. and Cour-Palais, B. G. (1978). Collision frequency of artificial satellites: The creation of a debris belt. *Journal of Geophysical Research*, 83(A6): 2637-2646.
- [19] Kessler, D. J., Johnson, N. L., Liou, J. C. and Matney, M. (2010). The Kessler syndrome: Implications to future space operations. AAS-10-016.
- [20] Koopmans, T. C. (1963). On the concept of optimal economic growth. Cowles Foundation Discussion Papers 12-1-1963.
- [21] Krusell, P. and Smith, A. A. (2024). Climate change around the world. Manuscript.
- [22] Lau, M. I., Pahlke, A. and Rutherford, T. F. (2002). Approximating infinity-horizon models in a complementarity format: A primer in dynamic general equilibrium analysis. *Journal of Economic Dynamics and Control*, 26(4): 577-609.

- [23] Liou, J. C. and Johnson, N. L. (2006). Risks in space from orbiting debris. *Science*, 311: 340–341.
- [24] Lucas, R. E. (2167). Adjustment costs and the theory of supply. *Journal of Political Economy*, 75(4-1): 321-334.
- [25] Manne, A. S. (1970). Sufficient conditions for optimality in an infinite horizon development plan. *Econometrica*, 38(1): 18-38.
- [26] Manne, A. S. (1977). *ETA-MACRO: A Model of Energy-economy Interactions*. Electric Power Research Institute.
- [27] Manne, A. S. and Richels, R. G. (1992). *Bying Greenhouse Insurance: The Economics Costs of CO2 Emission Limits*. MIT Press, Cambridge.
- [28] Manne, A. S., Mendelsohn, R. and Richels, R. (1995). MERGE: a model for evaluating regional and global effects of GHG reduction policies. *Energy Policy*, 23(1): 17-34.
- [29] Mercenier, J. and Michel, P. (1994). Discrete-time finite horizon approximation of infinite horizon optimization problems. *Econometrica*, 62(3): 635-656.
- [30] Nordhaus, W. D. (1992). An Optimal Transition Path for Controlling Greenhouse Gases. *Science*, 258(5086): 1315–1319.
- [31] Nordhaus, W. D. (1993). Rolling the ‘DICE’: an optimal transition path for controlling greenhouse gases. *Resource and Energy Economics*, 15(1): 27-50.
- [32] Nordhaus, W. D. (2008). *A Question of Balance: Weighing the Options on Global Warming Policies*. Yale University Press, New Haven and London.
- [33] Nordhaus, W. D. (2018). Projections and uncertainties about climate change in an era of minimal climate policies. *American Economic Journal. Economic Policy*, 10: 333–360.
- [34] Nordhaus, W. D. and Yang, Z. (1996). A regional dynamic general-equilibrium model of alternative climate change strategies. *American Economic Review*, 86(4): 741-765.
- [35] Nordhaus, W. D. and Boyer, J. (2000). *Warming the World: Economic Models of Global Warming*. MIT Press. Cambridge.
- [36] Nozawa, W., Kurita, K., Tamaki, T. and Managi, S. (2023). To what extent will space debris impact the economy? *Space Policy*, 66: 101580.
- [37] Peck, S. C. and Teisberg, T. J. (1992). CETA: A Model for Carbon Emissions Trajectory Assessment. *Energy Journal*, 0(1): 55-78.
- [38] Ramsey, F. (1928). A mathematical theory of saving. *Economic Journal*, 38: 543-559.
- [39] Rezai, A. (2011). The opportunity cost of climate policy: A question of reference. *Scandinavian Journal of Economics*, 113(4): 885-903.
- [40] Rezai, A. (2010). Recast the DICE and its policy recommendations. *Macroeconomic Dynamics*, 14: 275-289.
- [41] Rezai, A., Foley, D. K. and Taylor, L. (2012). Global warning and economic externalities. *Economic Theory*, 49: 329-351.

- [42] Rutherford, T. F. (1995). Extension of GAMS for complementarity problems arising in applied economic analysis. *Journal of Economic Dynamics and Control*, 19: 1299-1324.
- [43] Shiell, L. and Lyssenko, N. (2008). Computing business-as-usual with a representative agent and a pollution externality. *Journal of Economics Dynamics and Control*, 32: 1543-1568.
- [44] Stern, N. (2006). *The economics of climate change: The Stern Review*, Cambridge University Press.
- [45] Stoleru, L. G. (1965). An optimal policy for economic growth. *Econometrica*, 33(2): 321-348.
- [46] Yang, Z. (2003). Re-evaluation and renegotiation of climate change coalitions. A sequential closed-loop game approach. *Journal of Economic Dynamics and Control*, 27: 1563-1594. []

# On-line Supplementary Appendix for BUSINESS-AS-USUAL AND ORBITAL DEBRIS PATH

## APPENDIX A: DATA AND CALIBRATION

### A.1 *Data and initial values*

For the numerical simulations, we take 2023 as the initial period. Baseline values for this year are drawn from a variety of sources, including economic databases from the World Bank, International Monetary Fund (IMF), Penn World Table (PWT), Bureau of Economic Analysis (BEA), and the United Nations, as well as space activity databases from NASA, ESA, the Union of Concerned Scientists (UCS), Space-Track (U.S. Space Force), the Satellite Industry Association (SIA), the Space Foundation, and Jonathan C. McDowell.

Population (labor) in 2023 is taken from the United Nations Population Division, with a value of 8,056 million and an asymptotic population level of 10,200 million. The initial value of world GDP is drawn from the World Bank Economic Indicators, amounting to 184.65 trillion 2023 international US\$. The world capital stock is taken from the IMF Investment and Capital Stock Dataset (1960–2019) as the sum of private and public capital in 2019, with a value of 316.25 trillion 2017 international US\$. The corresponding estimate from the Penn World Table (PWT) is substantially higher, at 535.12 trillion 2017 international US\$ (Feenstra et al., 2015). Comparing the two databases reveals a large discrepancy in global capital stock estimates. Based on IMF data, the world capital-GDP ratio is 2.55, whereas the PWT implies a ratio of 4.26. Given this difference, and the fact that we need to split total capital into Earth capital and space capital, we rely on the Euler conditions for investment in Earth and space capital.

$$(1 + g_c)^\sigma = \beta \left( 1 - \delta_k + \alpha_1 \frac{y}{k} \right) \quad (1)$$

$$(1 + g_c)^\sigma (1 + g_q) = \beta \left( 1 - \delta_s + \alpha_2 (1 - m) \frac{y}{s} \right) \quad (2)$$

Using a per capita consumption growth rate of 2%, and given the calibration for  $\sigma$ ,  $\beta$ ,  $\alpha_1$ ,  $\alpha_2$ ,  $\delta_k$  and  $\delta_s$ ,  $m$ ,  $g_q$ , and the initial value of GDP, we find that  $k = 555.6987$  and  $s = 1.1959$  trillions international US\$. Hence, total initial world capital is 556.89, resulting in a capital-GDP ratio of 3.02, which is similar to standard values used in macroeconomic models. These values means that the ratio of space capital to Earth capital is 0.0022. Launch cost varies depending on the type of satellite and the orbit, ranging from a 10% to 60% of total cost. Initial launch cost as a fraction of space capital investment is fixed to be a 30% of total investment ( $m_{2023} = 0.30$ ).

The initial values for space-related variables are as follows. In 2023, there were 217 launches. The number of operational satellites in Earth orbit, reported by ESA for December 2023, was approximately 8,500. The initial stocks of derelict satellites and rocket bodies were estimated using the model's accumulation equations for the period 1957–2023. According to ESA, the number of derelict satellites in orbit in 2023 was about 3,500, while

## Appendix 2

NASA estimated 2,050 rocket bodies. The United States Space Surveillance Network (SSN) tracked a total of 31,150 pieces of debris. Most activity occurs in Low Earth Orbit (LEO, between 200 and 2,000 km) and Geostationary Orbit (GEO, at 35,786 km). Orbital debris is typically classified according to its size and whether it can be tracked with available technology. Projections from debris environment models, such as ESA's MASTER (Meteoroid and Space Debris Terrestrial Environment Reference) model and NASA's LEG-END (LEO-to-GEO Environment Debris Model), estimate approximately 36,500 debris fragments larger than 10 cm in diameter, around 1,000,000 objects between 1 cm and 10 cm, and more than 130 million fragments between 1 mm and 1 cm.

### A.2 Calibration of economic parameters

The calibration of economic parameters is carried out at the level of the world economy. While the United States remains the dominant spacefaring nation, with private space firms such as SpaceX playing a leading role, an increasing number of countries are developing space industries and acquiring launch capabilities, and the demand for satellite services is global. For this reason, the model is calibrated to an artificial world economy, where outer space is treated as an international common resource (Hardin, 1968).

Only a limited set of economic parameters requires calibration: the intertemporal preference parameter, the relative risk aversion parameter, the technological parameters of the production function, and the depreciation rates for physical capital and satellites. For these, we adopt standard values from the literature. In addition, the model incorporates two sources of technological progress: total factor productivity growth and investment-specific technological change in satellites.

The preference parameters are calibrated as follows. In the literature, the intertemporal elasticity of substitution parameter  $\sigma$  typically takes values between 1 (corresponding to a logarithmic instantaneous utility function) and 3. For example, Stern (2006) uses a value of 1, Nordhaus (2008) adopts 1.5, and Nordhaus (2017) employs 2. In our baseline calibration, we set  $\sigma = 1.5$ . For the pure intertemporal preference parameter, that is, the social rate of time preference, we follow the range of values commonly used in the climate-change literature. These range from 2% per year in Weitzman (2007) to 0.1% in Stern (2006). With a CRRA utility specification, the discount rate is given by  $r_t = \rho + \sigma g_{c,t}$ , where  $r_t$  is the discount rate and  $g_{c,t}$  the growth rate of consumption. Assuming a steady-state consumption growth rate of 2% and a relative risk aversion parameter of 2, this implies discount rates of about 6% (Nordhaus, 2017) and 4.1% (Stern, 2006), values broadly consistent with those used in standard dynamic stochastic general equilibrium models. In our baseline calibration, we set  $\rho = 1.5$  per year, following Nordhaus (2008).

Second, the calibration of technological parameters proceeds as follows. We fix the labor share at 0.65. Under constant returns to scale, the combined share of Earth capital and space capital is therefore 0.35 (i.e.,  $\alpha_1 + \alpha_2 = 0.35$ ). According to the Bureau of Economic Analysis (BEA, 2023), the U.S. space industry contributed \$129.9 billion (0.6% of GDP) in 2021 and employed about 360,000 workers. The Space Foundation (2023) reports that the global space economy was valued at \$546 billion in 2022, while the Satellite Industry Association (SIA, 2023) gives a figure of \$384 billion for the same year. Based on

this information, we split the capital share between Earth and space capital. The elasticity of output with respect to satellites is set to  $\alpha_2 = 0.35 \times 0.006 = 0.0021$ , which implies an elasticity of  $\alpha_1 = 0.3479$  for Earth capital. These values are consistent with Nozawa et al. (2023), who calibrate a Cobb–Douglas production function with labor, capital, and satellites and assign 0.002 to the elasticity of output with respect to satellites.

The depreciation rate for non-satellite capital,  $\delta_k$ , is fixed at the standard value of 0.07. Satellite depreciation is more uncertain, as lifetimes vary by type: from 6 months for CubeSats to about 15 years for GEO satellites, and 3–8 years for LEO satellites. Bongers and Torres (2023) assume an average lifetime of 8 years, corresponding to  $\delta_s = 0.1733$ , while Nozawa et al. (2023) use  $\delta_s = 0.216$ . In our calibration, we simulate the satellite accumulation equation for the period 1957–2023 to match ESA’s estimate of roughly 3,500 operational satellites in 2023. This yields a depreciation rate of  $\delta_s = 0.15$ .

Next, we calibrate the parameters driving the evolution of exogenous sources of growth. The initial TFP growth rate in 2023 is assumed to be 1.5% per year, decaying at 0.1% annually. The initial TFP level is computed as the ratio of initial output to the combined contribution of the three inputs. For investment-specific technological change (ISTC) in satellites, we follow a similar approach: the initial growth rate is set at 3% per year, with a decay rate of 0.5% annually. For launch costs, in the baseline calibration is fixed to the initial value. As an alternative, it is assumed that the initial growth rate is -0.5%, with a decay of 0.1% per year. Finally, the conversion parameter is calculated as the ratio of the initial number of active satellites in orbit to the corresponding stock value (in trillion US\$), yielding  $\mu = 7,107.6$ .

### A.3 Calibration of physical parameters

The calibration of physical parameters is as follows. First, the number of satellites per launch is calibrated by dividing the number of new satellites by the number of launches in the base year. In 2023, there were 217 launches, inserting a total of 2,950 satellites into orbit. While the ratio between launches and new satellites is changing rapidly due to the rise of small and micro-satellites and the increased payload capacity of modern launch systems, we assume this proportion remains constant for the future, giving  $\eta = 13.6$ .

The decay rate of debris fragments ( $\delta_f$ ) depends on several factors, including altitude, mass, area, solar activity, orbital circularity, and geomagnetic conditions. Estimates by the Australian Space Weather Agency (1999) indicate that the lifetime of space objects varies with altitude: roughly 1 day at 200 km, 1 month at 300 km, 1 year at 400 km, 10 years at 500 km, 100 years at 700 km, and 1,000 years at 900 km (King-Hele, 1987). Debris, however, is not uniformly distributed in altitude; spatial density data show that it is concentrated between 700 and 900 km (NASA, 2020).

The decay rate of debris fragments ( $\delta_f$ ) depends on multiple factors, including altitude, mass, area, solar activity, orbital circularity, and geomagnetic conditions. Estimates from the Australian Space Weather Agency (1999) indicate lifetimes varying from 1 day at 200 km to 1,000 years at 900 km (King-Hele, 1987), while debris is concentrated in the 700–900 km range (NASA, 2020). We also account for current orbital distributions: most activity is near 550 km due to the Starlink constellation, with sub-constellations planned

## Appendix 4

	Parameter	Definition	Value	Source
Economy	$\rho$	Pure preferences parameter	0.015	Nordhaus (2008)
	$\sigma$	Risk aversion parameter	1.500	Nordhaus (2008)
	$\alpha_1$	Capital share	0.3479	BEA
	$\alpha_2$	Satellite share	0.0021	BEA
	$\delta_k$	Capital depreciation rate	0.07	Standard
	$\delta_s$	Satellite depreciation rate	0.15	NASA
	$g_{a,0}$	Initial TFP growth rate	0.015	Assumption
	$g_{q,0}$	Initial satellite ISTC growth rate	0.030	Assumption
	$\delta_a$	TFP growth decay rate	0.001	Assumption
	$\delta_q$	ISTC growth decay rate	0.005	Assumption
	$g_{b,0}$	Launch cost change	-0.05	Assumption
	$\delta_b$	Launch cost change decay rate	0.01	Assumption
	$\zeta$	Population growth parameter	0.05	United Nations
	$\mu$	Conversion parameter	7,107.6	Internal
Space	$\eta$	Satellites per launch	13.6	NASA
	$\theta$	Collision risk parameter	$1.25 \times 10^{-10}$	ESA
	$\chi$	Fraction of abandoned satellites	0.40	ESA
	$\delta_f$	Fragment natural decay rate	0.01	NASA
	$\delta_w$	Derelict satellites natural decay rate	0.00015	Lafleur (2011)
	$\delta_z$	Rocket bodies natural decay rate	0.00015	Lafleur (2011)
	$\varepsilon_w$	Fraction of dead satellites breakups	0.0010	NASA
	$\varepsilon_z$	Fraction of body rocket breakups	0.0012	ESA
	$\varphi$	Body rockets per launch	0.60	ESA
	$\omega$	Fragments > 10 cm per launch	4	ESA
	$\phi_w$	Fragments > 10 cm per derelict satellite breakup	44.6	ESA
	$\phi_z$	Fragments > 10 cm per rocket body breakup	100.2	NASA/ESA
	$\gamma_s$	Fragments > 10 cm per operational satellite collision	70	NASA/ESA
	$\gamma_w$	Fragments > 10 cm per derelict satellite collision	70	NASA/ESA
$\gamma_z$	Fragments > 10 cm per rocket body collision	70	NASA/ESA	

TABLE A.1. Baseline calibration of the parameters of DISE-2024

at 340 km and 1,200 km, and the OneWeb constellation (658 satellites) at 1,200 km, where debris lifetimes can reach thousands of years. Alternative estimates in the literature vary. Nozawa et al. (2023) use 0.0067 based on Bongers and Torres (2023), assuming a 150-year average lifetime, similar to the FADE model estimate of 0.0062 (Lewis et al., 2009). Rao and Rondina (2025) use 0.074. Lafleur (2011) calculates LEO decay rates using ballistic coefficients and solar activity: under solar maximum, the average lifetime is 46.9 years (decay rate 0.021); under solar minimum, 332.8 years (decay rate 0.003), yielding a weighted mean of 0.012. Based on these data, we set  $\delta_f = 0.01$  in the baseline model, corresponding to a 1% annual decay rate, approximately representing an average orbit of 750 km.

The natural decay rates of derelict satellites ( $\delta_w$ ) and rocket bodies ( $\delta_z$ ) are typically lower than those of debris fragments due to their larger mass and surface area. Decay is strongly influenced by the mass-to-surface ratio: Lafleur (2011) estimates  $1.8 \text{ kg}/\text{m}^2$  for fragments versus  $110 \text{ kg}/\text{m}^2$  for satellites. Using the weighted distribution of satellites across orbital altitudes, Lafleur (2011) finds that the average lifetime of derelict satellites ranges from 3,990 years (decay rate 0.00025 under solar-maximum conditions) to 24,850

years (decay rate 0.00004 under solar-minimum conditions), yielding an average LEO decay rate of 0.000145. Assuming a similar mass-to-surface ratio for rocket bodies, we set  $\delta_w = \delta_z = 0.00015$ .

To calibrate the risk of collision ( $\theta$ ), we focus on debris larger than 1 cm, as such fragments can cause catastrophic damage to satellites. Collisions between operational satellites also occur, though some can be avoided by maneuvering; however, many satellites lack rapid or any maneuver capability. Farinella and Cordelli (1991) estimated  $\theta = 3 \times 10^{-10}$  for an estimated 50,000 debris objects, implying roughly 0.2 satellite losses per year (probability of collision  $\theta \times 50,000 = 1.5 \times 10^{-5}$ ). Kawamoto et al. (2019) report higher probabilities: for debris >10 cm, the total collision probability is about 0.1 for 800–900 km orbits, 0.05 for 900–1,000 km, and 0.025 for 600–700 km. Following Farinella and Cordelli (1991) and historical observations (four collisions between 1991 and 2009), we adopt a reference total collision probability of 0.2, roughly one fatal collision every five years, yielding  $\theta \times D = 6.6 \times 10^{-5}$ . Other estimates include Lafleur (2011) at  $6.895 \times 10^{-10}$ , Percy (2015) at  $6.37 \times 10^{-10}$ , Bongers and Torres (2023) at  $6.37 \times 10^{-11}$ , and Guyot and Rouillon (2024) at  $4 \times 10^{-10}$ . For the baseline calibration, we use  $\theta = 1.25 \times 10^{-10}$ , corresponding to a collision probability  $\theta \times D_{1,t} = 1.25 \times 10^{-4}$ .

The operational life of satellites is relatively short, and defunct satellites abandoned in orbit are an important source of orbital debris. This occurs when satellites run out of fuel and cannot be moved to graveyard orbits; once non-operational, they automatically become debris. Such cases were common in the early stages of space activity. Abandoned satellites pose significant risks due to their mass, as illustrated by the 2009 collision of the derelict Kosmos-2251 with the operational Iridium-33.

Although the number of abandoned satellites is small relative to other forms of debris, NASA tracks 3,524 derelict satellites in 2023, from which we estimate the fraction of abandoned satellites ( $\chi$ ) to be 0.40. This fraction is expected to decline over time due to improved international standards requiring reserve fuel for de-orbiting maneuvers.

The fraction of rocket bodies per launch ( $\varphi$ ) left in orbit is estimated at 0.6, consistent with the number of abandoned rocket bodies in 2023 (McDowell, 2024). The fractions of dead satellite breakups ( $\delta_w$ ) and rocket body breakups ( $\delta_z$ ) are calibrated to match the derelict satellites and rocket bodies estimated by NASA and ESA for 2023, yielding 0.001 and 0.0012, respectively.

The number of debris pieces per launch ( $\omega$ ) is the primary source of new fragments, including only parts discarded during satellite insertion (excluding rocket bodies). To match the number of tracked objects (>10 cm) in orbit, we calibrate  $\omega = 4$ . All fragment law-of-motion parameters are calibrated based on debris larger than 10 cm, then scaled to account for smaller fragments (>1 cm).

Finally, we calibrate the number of fragments produced per collision and per breakup. The number of fragments per collision of operational satellites, derelict satellites, and rocket bodies ( $\gamma_s$ ,  $\gamma_w$ , and  $\gamma_z$ , respectively) and per breakup of derelict satellites and rocket bodies ( $\phi_w$  and  $\phi_z$ ) is based on estimates from the NASA Breakups Database (Anz-Meador et al., 2022), which documents on-orbit breakups, collisions, and anomalous events through 15 April 2022. The database records 268 fragmentation events and 87

## Appendix 6

anomalous events, including 6 debris-causing collisions, 83 rocket body breakups, and 51 satellite self-destructions.

For operational satellite collisions, the database reports six events producing 2,430 cataloged debris (average 347 per collision). The DISCOS database reports five collisions, averaging 483.6 fragments. Farinella and Cordelli (1991) assume two unintentional explosions per year, producing 2,059 fragments  $>1$  cm per year. Lewis et al. (2009) estimate 625 fragments per catastrophic collision ( $>10$  cm) and 25 per damaging collision (1–10 cm). Scaling to debris  $>1$  cm, a catastrophic collision yields 17,748 fragments, and a non-catastrophic collision yields 710. Based on these estimates, we set  $\gamma_s = 70$ .

Due to limited data, we assume derelict satellites and rocket bodies produce the same number of fragments per collision as operational satellites ( $\gamma_w = \gamma_z = 70$ ). Although differences in mass and structure could affect fragmentation, sensitivity analyses with  $\gamma_z$  ranging from 50 to 200 show similar dynamics and consistent conclusions.

For debris generated by breakups, NASA's database reports 47 satellite breakups (excluding anti-satellite or self-destruction events), producing 2,289 cataloged fragments, an average of 44.6 fragments per derelict satellite breakup ( $\phi_w = 44.6$ ). For rocket bodies, 83 breakups produced 8,315 cataloged debris, giving an average of 100.2 fragments per breakup ( $\phi_z = 100.2$ ).

### APPENDIX B: CENTRAL PLANNER PROBLEM

This appendix presents the planning problem in which a central planner maximizes social welfare. The central planner chooses consumption, investment in Earth capital, and investment in satellites, to maximize social welfare. This is a first best, where the negative externality is fully internalized. The maximization problem solved by the central planner is given by,

$$\max_{c_t, i_t^k, i_t^s, D_t} E_0 \sum_{t=0}^{\infty} \beta^t U(\hat{c}_t) N_t \quad (\text{B.1})$$

subject to

$$c_t + i_t^k + i_t^s = y_t \quad (\text{B.2})$$

$$y_t = a_t f(k_t, s_t, N_t) \quad (\text{B.3})$$

$$k_{t+1} = (1 - \delta_k)k_t + i_t^k \quad (\text{B.4})$$

$$i_t^s = h_t + l_t \quad (\text{B.5})$$

$$l_t = m_t i_t^s \quad (\text{B.6})$$

$$s_{t+1} = (1 - \delta_s)s_t + q_t(1 - m_t)i_t^s - x_t \quad (\text{B.7})$$

$$x_t = (1 - v_t)\theta D_{2,t} s_t \quad (\text{B.8})$$

$$D_{i,t} = W_t + Z_t + F_{i,t} \quad i = 1, 2, 3 \quad (\text{B.9})$$

$$W_{t+1} = (1 - \delta_w - \varepsilon_w)W_t - \theta(D_{2,t} + (1 - v_t)S_t)W_t + \chi\delta_s S_t \quad (\text{B.10})$$

$$Z_{t+1} = (1 - \delta_z - \varepsilon_z)Z_t - \theta(D_{2,t} + (1 - v_t)S_t)Z_t + \phi L_t \quad (\text{B.11})$$

$$F_{1,t+1} = (1 - \delta_f)F_{1,t} + \omega L_t + \phi_w \varepsilon_w W_t + \phi_z \varepsilon_z Z_t + \gamma_s X_t + \gamma_w D_{2,t} W_t + \gamma_z D_{2,t} Z_t \quad (\text{B.12})$$

$$L_t = \frac{\mu}{\eta} h_t \quad (\text{B.13})$$

$$X_t = \mu \frac{x_t}{q_t} \quad (\text{B.14})$$

$$F_{2,t} = (1 + \Gamma)F_{1,t} \quad (\text{B.15})$$

Additionally, the mapping from the "economic" model to the "physical" model is given by the following expressions:

$$X_t = (1 - v_t)\theta D_{2,t} S_t \quad (\text{B.16})$$

$$S_t = \mu \frac{s_t}{q_t} \quad (\text{B.17})$$

$$H_t = \eta L_t \quad (\text{B.18})$$

The maximization problem can be defined as:

$$\begin{aligned} \mathcal{L} = E_t \sum_{t=0}^{\infty} \beta^t U(\hat{c}_t) N_t & \\ - \sum_{t=0}^{\infty} \lambda_{1,t} \left[ c_t + k_{t+1} - (1 - \delta_k)k_t + \frac{\eta}{\mu(1 - m_t)} L_t - a_t f(k_t, s_t, N_t) \right] & \\ - \sum_{t=0}^{\infty} \lambda_{2,t} [x_t - (1 - v_t)\theta D_{2,t} S_t] & \\ - \sum_{t=0}^{\infty} \lambda_{3,t} \left[ s_{t+1} - (1 - \delta_s)s_t - \frac{\eta}{\mu} q_t L_t + x_t \right] & \\ - \sum_{t=0}^{\infty} \lambda_{4,t} [D_{2,t} - W_t - Z_t - (1 + \Gamma)F_{1,t}] & \\ - \sum_{t=0}^{\infty} \lambda_{5,t} [W_{t+1} - (1 - \delta_w - \varepsilon_w)W_t + \theta(D_{2,t} + (1 - v_t)S_t)W_t - \chi \delta_s S_t] & \\ - \sum_{t=0}^{\infty} \lambda_{6,t} [Z_{t+1} - (1 - \delta_z - \varepsilon_z)Z_t + \theta(D_{2,t} + (1 - v_t)S_t)Z_t - \phi L_t] & \\ - \sum_{t=0}^{\infty} \lambda_{7,t} [F_{1,t+1} - (1 - \delta_f)F_{1,t} - \omega L_t - \phi_w \varepsilon_w W_t - \phi_z \varepsilon_z Z_t & \\ - \gamma_s X_t - \gamma_w \theta D_{2,t} W_t - \gamma_z \theta D_{2,t} Z_t] & \quad (\text{B.19}) \end{aligned}$$

The Lagrangian multipliers for each constraint in period  $t$  are  $\lambda_{1,t}$ ,  $\lambda_{2,t}$ ,  $\lambda_{3,t}$ ,  $\lambda_{4,t}$ ,  $\lambda_{5,t}$ ,  $\lambda_{6,t}$ , and  $\lambda_{7,t}$ .  $\lambda_{1,t}$  is the standard shadow price of consumption.  $\lambda_{2,t}$  is the cost of the probability of collision.  $\lambda_{3,t}$  is the price of satellite assets.  $\lambda_{4,t}$  is the cost of the stock of

## Appendix 8

orbital debris, and  $\lambda_{5,t}$ ,  $\lambda_{6,t}$ , and  $\lambda_{7,t}$  represents the shadow cost of derelict satellites, rocket bodies, and fragments, respectively.

First order conditions from the maximization problem, for  $t = 0, 1, \dots, \infty$  are,

$$\frac{\partial \mathcal{L}}{\partial c_t} = \beta^t U'(c_t) - \lambda_{1,t} = 0 \quad (\text{B.20})$$

$$\frac{\partial \mathcal{L}}{\partial k_{t+1}} = -\lambda_{1,t} + \lambda_{1,t+1} [1 - \delta_k + a_{t+1} f'_k(k_{t+1}, s_{t+1}, N_{t+1})] = 0 \quad (\text{B.21})$$

$$\begin{aligned} \frac{\partial \mathcal{L}}{\partial s_{t+1}} = & \lambda_{1,t+1} a_{t+1} f'_s(k_{t+1}, s_{t+1}, N_{t+1}) + \lambda_{2,t} (1 - v_t) \theta D_{2,t+1} - \lambda_{3,t} + \lambda_{3,t+1} (1 - \delta_s) \\ & - \lambda_{5,t+1} \frac{\mu}{q_{t+1}} [\theta (1 - v_{t+1}) W_{t+1} - \chi \delta_s] - \lambda_{6,t+1} \frac{\mu \theta (1 - v_{t+1}) Z_{t+1}}{q_{t+1}} = 0 \end{aligned} \quad (\text{B.22})$$

$$\frac{\partial \mathcal{L}}{\partial L_t} = -\lambda_{1,t} \frac{\eta}{\mu(1 - m_t)} + \lambda_{3,t} \frac{\eta q_t}{\mu} + \lambda_{6,t} \varphi + \lambda_{7,t} \omega = 0 \quad (\text{B.23})$$

$$\frac{\partial \mathcal{L}}{\partial x_t} = -\lambda_{2,t} - \lambda_{3,t} + \lambda_{7,t} \frac{\gamma_s \mu}{q_t} = 0 \quad (\text{B.24})$$

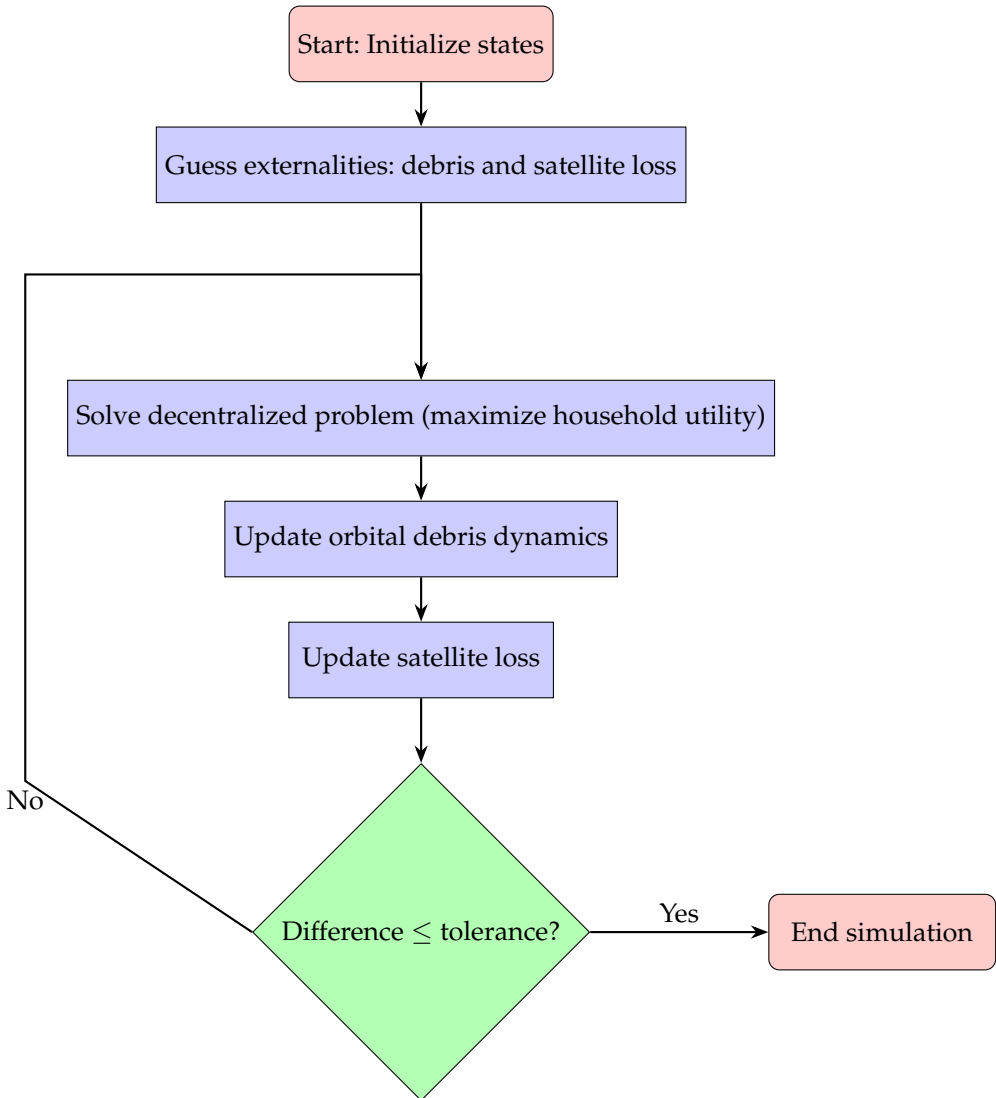
$$\frac{\partial \mathcal{L}}{\partial D_{2,t}} = \lambda_{2,t} \theta (1 - v_t) s_t - \lambda_{4,t} - \lambda_{5,t} \theta W_t - \lambda_{6,t} \theta Z_t + \lambda_{7,t} [\gamma_w \theta W_t + \gamma_z \theta Z_t] = 0 \quad (\text{B.25})$$

$$\begin{aligned} \frac{\partial \mathcal{L}}{\partial W_{t+1}} = & \lambda_{4,t+1} - \lambda_{5,t} + \lambda_{5,t+1} [1 - \delta_w - \varepsilon_w - \theta (D_{2,t+1} + (1 - v_{t+1}) S_{t+1})] \\ & + \lambda_{7,t+1} [\phi_w \varepsilon_w + \gamma_w \theta D_{2,t}] = 0 \end{aligned} \quad (\text{B.26})$$

$$\begin{aligned} \frac{\partial \mathcal{L}}{\partial Z_{t+1}} = & \lambda_{4,t+1} - \lambda_{6,t} + \lambda_{6,t+1} [1 - \delta_z - \varepsilon_z - \theta (D_{2,t+1} + (1 - v_{t+1}) S_{t+1})] \\ & + \lambda_{7,t+1} [\phi_z \varepsilon_z + \gamma_z \theta D_{2,t}] = 0 \end{aligned} \quad (\text{B.27})$$

$$\frac{\partial \mathcal{L}}{\partial F_{1,t+1}} = \lambda_{4,t+1} (1 + \Gamma) - \lambda_{7,t} + \lambda_{7,t+1} (1 - \delta_f) = 0 \quad (\text{B.28})$$

## APPENDIX C: FLOW CHART OF THE FIXED POINT ALGORITHM



## REFERENCES

- [1] Anz-Meador P, Opiela J, Liou JC (2022) History of on-orbit satellite fragmentation, 16th edn. NASA
- [2] Australian Space Weather Agency. 1999. *Satellite orbital decay calculations*. Sidney: Australia.
- [3] Bongers, A. and Torres, J. L. (2023). Orbital debris and the market for satellites. *Ecological Economics*, 209: 107831.
- [4] Bureau of Economic Analysis (2023). *Space Economy Data, 2012-2021*.
- [5] Farinella, P. and Cordelli, A. (1991). The proliferation of orbiting fragments: a simple mathematical model. *Science and Global Security*, 2: 365-378.
- [6] Feenstra, R. C., Inklaar, R. and Timmer, M. P. (2015). The Next Generation of the Penn World Table. *American Economic Review*, 105(10): 3150-3182.
- [7] Guyot, J. and Rouillon, S. (2024). Sustainable management of space activity in low Earth orbit. *Journal of Environmental Economics and Policy*, 13(2): 188-212.
- [8] Kawamoto, S., Nagaoka, N., Sato, T. and Hanada, T. (2019). Impact on collision probability by post mission disposal and Active Debris Removal. First International Orbital Debris Conference.
- [9] King-Hele, D. G. (1987). *Satellite orbits in an atmosphere: theory and application*. Springer Netherlands.
- [10] Lafleur, J.L. (2011). Extension of a simple mathematical model for orbital debris proliferation and mitigation. *American Astronautical Society*, 11-173.
- [11] Lewis, H.G., Swinerd, G.G., Newland, R.J. and Saunders, A. (2009). The fast debris evolution model. *Advances in Space Research*, 44: 568-578.
- [12] McDowell, J. (2024). *Space Activities 2023*. Jonathan's Space Report.
- [13] NASA (2020). The tracked objects in Low Earth Orbit: 2000–2020. *Orbital Debris Quarterly Review*, 24(4): 11.
- [14] Nordhaus, W. D. (2008). *A Question of Balance: Weighing the Options on Global Warming Policies*. Yale University Press, New Haven and London.
- [15] Nordhaus, W. D. (2017). Revisiting the social cost of carbon. *Proceedings of the National Academy of Sciences*, 114(7): 1518-1523.
- [16] Nozawa, W., Kurita, K., Tamaki, T. and Managi, S. (2023). To what extent will space debris impact the economy? *Space Policy*, 66: 101580.
- [17] Percy, T. (2015). *Simplified population growth modelling for low earth orbit*. Dissertations, 76. University of Alabama.
- [18] Rao, A, and Rondina, G. (2025). The economics of orbit use: Open access, external costs, and runaway debris growth. *Journal of the Association of Environmental and Resource Economists*, 12(2): 353-388.

- [19] Satellite Industry Association (2023). *SIA Reports Record Growth for the Satellite Industry in 2023*.
- [20] Space Foundation (2023). *The Space Report 2023 Q2*.
- [21] Stern, N. (2006). *The economics of climate change: The Stern Review*, Cambridge University Press.
- [22] Weitzman, M. L. (2007). A review of the Stern Review on the economics of climate change. *Journal of Economic Literature*, 45: 703–724. []